HAL
open science

# FINITE VOLUME SCHEMES FOR DIFFUSION EQUATIONS: INTRODUCTION TO AND REVIEW OF MODERN METHODS

Jerome Droniou

▶ **To cite this version:**

Jerome Droniou. FINITE VOLUME SCHEMES FOR DIFFUSION EQUATIONS: INTRODUCTION TO AND REVIEW OF MODERN METHODS. Mathematical Models and Methods in Applied Sciences, 2014, 24 (8), pp.1575-1619. 10.1142/S0218202514400041 . hal-00813613v3

**HAL Id: hal-00813613**

**https://hal.science/hal-00813613v3**

Submitted on 7 Feb 2014

**HAL** is a multi-disciplinary open access archive for the deposit and dissemination of scientific research documents, whether they are published or not. The documents may come from teaching and research institutions in France or abroad, or from public or private research centers.

L'archive ouverte pluridisciplinaire **HAL**, est destinée au dépôt et à la diffusion de documents scientifiques de niveau recherche, publiés ou non, émanant des établissements d'enseignement et de recherche français ou étrangers, des laboratoires publics ou privés.

# FINITE VOLUME SCHEMES FOR DIFFUSION EQUATIONS: INTRODUCTION TO AND REVIEW OF MODERN METHODS

JEROME DRONIOU

*School of Mathematical Sciences, Monash University*
*Victoria 3800, Australia.*

*jerome.droniou@monash.edu*

We present Finite Volume methods for diffusion equations on generic meshes, that received important coverage in the last decade or so. After introducing the main ideas and construction principles of the methods, we review some literature results, focusing on two important properties of schemes (discrete versions of well-known properties of the continuous equation): coercivity and minimum-maximum principles. Coercivity ensures the stability of the method as well as its convergence under assumptions compatible with real-world applications, whereas minimum-maximum principles are crucial in case of strong anisotropy to obtain physically meaningful approximate solutions.

*Keywords*: review, elliptic equation, finite volume schemes, multi-point flux approximation, hybrid mimetic mixed methods, discrete duality finite volume schemes, coercivity, convergence analysis, monotony, minimum and maximum principles.

AMS Subject Classification: 65N06, 65N08, 65N12, 65N15, 65N30

## 1. Introduction

Diffusion processes are ubiquitous in physics of flows, such as heat propagation or flows in porous media encountered in reservoir engineering. A simple form of diffusion equation is

$$\begin{aligned} &-\mathrm{div}(\Lambda(x)\nabla\overline{u}(x)) = f(x)\,, && x\in\Omega,\\ &\overline{u}(x) = \overline{u}_b\,, && x\in\partial\Omega, \end{aligned} \tag{1.1}$$

where $\Omega$ is the domain of study, $f$ describes the volumic sources or sinks, $\Lambda$ encodes the diffusion properties of the medium, $\overline{u}_b$ is the fixed boundary condition and $\overline{u}$ is the unknown of interest (pressure, saturation, etc.). Although very simplified with respect to real-world models, Equation (1.1) already contains some of the main issues that have to be dealt with when designing and analysing numerical methods for diffusion processes. The assumptions on the data are:

$$\Omega \text{ is a bounded connected polygonal open subset of } \mathbb{R}^d,\ d\geq 1, \tag{1.2}$$

$$f\in L^2(\Omega)\,,\quad \overline{u}_b\in H^{1/2}(\Omega)\,, \tag{1.3}$$

$$\begin{aligned} &\Lambda:\Omega\to\mathbb{R}^{d\times d} \text{ is symmetric-valued, essentially bounded and coercive}\\ &\text{(i.e. } \exists\lambda_-,\lambda_+>0 \text{ such that, for a.e. } x\in\Omega \text{ and all } \xi\in\mathbb{R}^d,\\ &\lambda_-|\xi|^2\leq\Lambda(x)\xi\cdot\xi\leq\lambda_+|\xi|^2) \end{aligned} \tag{1.4}$$

($\cdot$ and $|\cdot|$ are the Euclidean dot product and norm on $\mathbb{R}^d$). No other regularity properties are assumed on $\Lambda$, $f$ or $\overline{u}_b$, and the proper mathematical formulation of (1.1) is therefore, denoting by $\gamma : H^1(\Omega) \mapsto H^{1/2}(\partial\Omega)$ the trace operator:

$$\begin{aligned} &\overline{u} \in \{v \in H^1(\Omega) \ : \ \gamma(v) = \overline{u}_b\}, \\ &\forall \varphi \in H^1_0(\Omega)\,, \quad \int_\Omega \Lambda(x)\nabla\overline{u}(x)\cdot\nabla\varphi(x)\mathrm{d}x = \int_\Omega f(x)\varphi(x)\mathrm{d}x. \end{aligned} \tag{1.5}$$

Amongst the numerous families of numerical methods for diffusion equations (Finite Difference, Finite Element, Discontinuous Galerkin...), Finite Volume (FV) schemes are methods of choice for a number of engineering applications in which the conservation of various extensive quantities is important. Local conservativity of the fluxes is in particular essential to handle the hyperbolicity and strong coupling which occur in models of miscible or immiscible flows in porous media.

The purpose of this work is to present a few modern FV methods for (1.1) and to review some of the mathematical results established for these methods. Although FV methods can be applied on a number of fluid models, our discussion will be made with models of porous media flows in mind. In this case, (1.1) corresponds to a steady single-phase single-component Darcy problem with no gravitational effects, $\overline{u}$ is the pressure and $\Lambda$ is the permeability field[45].

The paper is organised as follows. In the rest of this section, we detail the basics behind the construction of FV methods and we point out two important properties of Equation (1.1) (coercivity and minimum-maximum principle) which are also desirable for discretisations thereof. Coercivity, in particular, is at the core of techniques which allows one to carry out convergence proofs without assuming non-physical regularities on the data or the solution. Sec. 2 presents the most classical FV method for (1.1), based on a 2-point flux approximation, and highlights its coercivity and minimum-maximum principle properties as well as its main flaw: it is hardly applicable on meshes encountered in practical applications. Secs. 3, 4 and 5 then present three families of FV schemes applicable on generic meshes: Multi Point Flux Approximation methods (O-, L- and G-methods), Hybrid Mimetic Mixed methods (including Hybrid Finite Volume methods, Mimetic Finite Difference schemes and Mixed Finite Volume methods) and Discrete Duality Finite Volume methods. In each of these sections, we first present the construction of the method, focusing on its principles rather than on the details of the computations, and we then review the literature results on their coercivity (and convergence) and minimum-maximum principle properties. These sections are also completed by short conclusions summarising the strengths and weaknesses of each method. In Sec. 6, we consider some FV schemes specifically designed to satisfy minimum-maximum principles on any mesh. Sec. 7 concludes the paper.

### 1.1. *What is a Finite Volume scheme?*

Good question... not easy to answer given the number of methods presented in the literature as "Finite Volume" schemes. Nevertheless, some basic ideas remain which

should be shared by any method called "Finite Volume".

The physical principle that leads to (1.1) is the balance of some extensive quantity $Q$ (heat, component mass, etc.): given a domain $\omega$, the variation of $Q$ inside $\omega$ comes from the creation of $Q$ in $\omega$ and the transfer of $Q$ through $\partial\omega$. In a stationary context, there is no variation of $Q$ and the volumic creation inside $\omega$ must therefore balance out the quantity of $Q$ which leaves $\omega$ through $\partial\omega$. Under modelling assumptions, the creation of $Q$ inside $\omega$ has a volumetric density function $f$ and the flow of $Q$ outside $\omega$ has a surfacic density $-\Lambda(x)\nabla\overline{u}(x)\cdot\mathbf{n}_\omega(x)$ (Darcy's or Fourier's law), where $\mathbf{n}_\omega$ is the outer unit normal to $\partial\omega$ and $\Lambda(x)$ is a symmetric positive definite matrix — heat conductivity matrix in the case of the heat equation, permeability matrix in reservoir engineering. The mass balance of $Q$ then reads

$$\int_{\partial\omega} -\Lambda(x)\nabla\overline{u}(x)\cdot\mathbf{n}_\omega(x)\mathrm{d}S(x) = \int_\omega f(x)\mathrm{d}x. \tag{1.6}$$

Using Stokes' formula on the left-hand side, taking $\omega$ a ball around $x\in\Omega$, dividing by the measure of $\omega$ and letting its radius tend to 0 leads to (1.1). This is the "infinitesimal" control volume technique to derive the diffusion equation.

If, on the other hand, we consider a "finite" control volume approach in which $\omega = K$ is a (small but not infinitesimal) polygonal open set, then (1.6) becomes

$$\sum_{\sigma \text{ edge of } K} \overline{F}_{K,\sigma} = \int_K f(x)\mathrm{d}x \tag{1.7}$$

where $\overline{F}_{K,\sigma} = \int_\sigma -\Lambda(x)\nabla\overline{u}(x)\cdot\mathbf{n}_K(x)\mathrm{d}S(x)$ is the flux of $\overline{u}$ through $\sigma$. It can also be noticed that, if $\sigma$ is an edge between two polygons $K$ and $L$, then

$$\overline{F}_{K,\sigma} + \overline{F}_{L,\sigma} = 0. \tag{1.8}$$

**Remark 1.1.** Another way to get (1.7) is to integrate (1.1) on $K$. This is how FV methods are usually presented in textbooks, but it is important to realise that (1.7) directly comes from physical principles (without even writing (1.1)). This explains why FV methods are particularly attractive in many engineering contexts.

The balance (1.7) and conservativity (1.8) of the fluxes are the two main elements on which FV methods are built. Let $(\mathcal{M},\mathcal{E},\mathcal{P})$ be a mesh of $\Omega$ as given by Definition 1.1 below. All FV methods we consider here have at least cell unknowns $(u_K)_{K\in\mathcal{M}}$, that play the role of approximate values of $(\overline{u}(\boldsymbol{x}_K))_{K\in\mathcal{M}}$. Such cell unknowns are often desirable in applications, for coupling issues and because the medium properties (permeability, etc.) are usually constant in each cell. Some FV methods also use additional unknowns, e.g. approximate values of $\overline{u}$ on the edges. The principle of FV schemes is to compute, using all these unknowns, consistent approximations $F_{K,\sigma}$ of $\overline{F}_{K,\sigma}$ and to write discrete versions of (1.7) and (1.8):

$$\text{for any } K\in\mathcal{M}\ :\ \sum_{\sigma\in\mathcal{E}_K} F_{K,\sigma} = \int_K f(x)\mathrm{d}x, \tag{1.9}$$

$$\text{for any edge } \sigma \text{ between two distinct } K,L\in\mathcal{M}\ :\ F_{K,\sigma}+F_{L,\sigma}=0. \tag{1.10}$$

**Definition 1.1 (Mesh).** A mesh of $\Omega$ is $(\mathcal{M}, \mathcal{E}, \mathcal{P})$ where:

- $\mathcal{M}$ is a finite family of non-empty open disjoint polygons (the "control volumes" or "cells") such that $\overline{\Omega} = \cup_{K\in\mathcal{M}} \overline{K}$,
- $\mathcal{E}$ is a finite family of non-empty disjoint planar subsets of $\Omega$ (the "edges") with positive $(d-1)$-dimensional measure. We assume that for each control volume $K$ there exists $\mathcal{E}_K \subset \mathcal{E}$ such that $\partial K = \cup_{\sigma\in\mathcal{E}_K} \overline{\sigma}$. We also assume that each edge $\sigma \in \mathcal{E}$ belongs to exactly one or two sets $(\mathcal{E}_K)_{K\in\mathcal{M}}$.
- $\mathcal{P}$ is a family of points $(\boldsymbol{x}_K)_{K\in\mathcal{M}}$ such that, for each $K$, $\boldsymbol{x}_K \in K$.

We denote by $|K|$ the $d$-dimensional measure of $K \in \mathcal{M}$, by $|\sigma|$ the $(d-1)$-dimensional measure of $\sigma \in \mathcal{E}$ and by $\mathbf{n}_{K,\sigma}$ the unit normal to $\sigma \in \mathcal{E}_K$ outward $K$. We also partition $\mathcal{E}$ into the interior edges $\mathcal{E}_{\text{int}}$ (those included in $\Omega$) and the exterior edges $\mathcal{E}_{\text{ext}}$ (those included in $\partial\Omega$). The size of the mesh is $h_{\mathcal{M}} = \max_{K\in\mathcal{M}} \text{diam}(K)$. We also take $\Lambda_K$ a value of $\Lambda$ in $K$ (e.g. $\frac{1}{|K|}\int_K \Lambda$ or $\Lambda(\boldsymbol{x}_K)$ – in reservoir applications, $\Lambda$ is constant in each cell $K$).

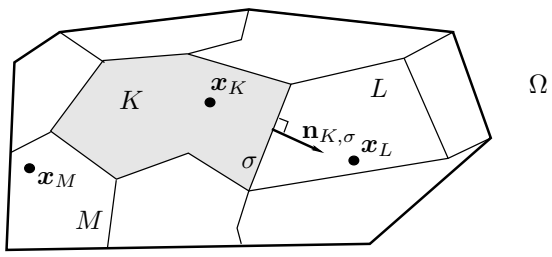


Fig. 1. A mesh of $\Omega$.

**Remark 1.2.** Although we use a 2D vocabulary (polygon, edges...), most of what we present here is valid in any space dimension.

### 1.2. *Convergence analysis and coercivity*

In reservoir applications, the data (and thus the solution) are not smooth. It is for example natural for the permeability $\Lambda$ to be discontinuous from one geological layer to another. Convergence analysis of numerical methods for such problems should take into account these practical constraints and should therefore not rely on non-physical regularity assumptions on the data or solution. Being able to carry out a convergence analysis under very weak regularity assumptions on the data or the solution is also essential for more complex models (Navier-Stokes equations, multi-phase flows, etc.).

Assuming to simplify that $\overline{u}_b = 0$ (in which case $\overline{u} \in H_0^1(\Omega)$), an efficient path to prove the convergence of FV methods for (1.1) is to follow these steps:

(C1) Establish *a priori* energy estimates on the solution to the scheme, in a mesh- and scheme-dependent discrete norm which mimics the $H_0^1$ norm,
(C2) Prove a discrete Rellich compactness result, i.e. that, as the mesh size tends to 0, sequences of approximate solutions bounded in these discrete norms have subsequences which converge([a]) to some function $\overline{u} \in H_0^1(\Omega)$,
(C3) Prove that any such limit $\overline{u}$ of approximate solutions satisfies (1.5).

Because the solution to (1.5) is unique, Steps (C1)—(C3) show the convergence of the scheme in the sense that the whole sequence of approximate solutions converges to the solution of (1.5). Moreover, for linear schemes, Step (C1) ensures the existence and uniqueness of a solution to the scheme.

Following this path does not require any regularity property on $\Lambda$, $f$ or $\overline{u}$ besides those in (1.2)—(1.4) and (1.5). Ensuring that *a priori* energy estimates can be obtained in a proper "discrete $H_0^1$ norm" however requires some assumptions on the scheme. Consider the continuous equation (1.1), multiply it by $\overline{u}$ and integrate by parts (or, equivalently, take $\varphi = \overline{u}$ in (1.5)). Then

$$\lambda_- |\overline{u}|^2_{H_0^1} \leq \int_\Omega \Lambda(x)\nabla\overline{u}(x)\cdot\nabla\overline{u}(x)\mathrm{d}x = \int_\Omega f(x)\overline{u}(x)\mathrm{d}x \leq ||f||_{L^2}||\overline{u}||_{L^2} \tag{1.11}$$

and the Poincaré inequality $||\overline{u}||_{L^2(\Omega)} \leq \mathrm{diam}(\Omega)|\overline{u}|_{H_0^1(\Omega)}$ gives estimate on $|\overline{u}|_{H_0^1(\Omega)} := ||\,|\nabla\overline{u}|\,||_{L^2(\Omega)}$. The key element here is the coercivity of $\Lambda$ (which is equivalent to the coercivity of the bilinear form in (1.5)). Discrete $H_0^1$ estimates on the solution to a FV scheme are usually obtained by mimicking this process at the discrete level: multiply the scheme by the unknown, perform discrete integration by parts (or, equivalently, take the unknown as test function in a variational formulation of the scheme) and conclude by establishing a discrete Poincaré inequality (see e.g. Sec. 2.1). This process does not work for all schemes but, when it does, it shows how to find the discrete $H_0^1$ norm associated with the scheme and mesh. For schemes using only cell unknowns, for example, multiplying (1.9) by $u_K$, summing on the cells and using (1.10), we see that a discrete version of (1.11) can be obtained if there exists a discrete $H_0^1$ norm $||.||_{1,\mathrm{disc}}$ satisfying the Poincaré's inequality

$$\left(\sum_{K\in\mathcal{M}} |K|u_K^2\right)^{1/2} \leq C||u||_{1,\mathrm{disc}}$$

and the estimate

$$||u||^2_{1,\mathrm{disc}} \leq C\sum_{\sigma\in\mathcal{E}} F_{K,\sigma}(u_K - u_L), \tag{1.12}$$

for some $C$ not depending on $u$ or the mesh (in the previous sum, $K, L$ are the cells on each side of $\sigma \in \mathcal{E}_{\mathrm{int}}$ and $u_L = 0$ if $\sigma \in \mathcal{E}_{\mathrm{ext}} \cap \mathcal{E}_K$).

[a]In a sense depending on the method, but which includes at least some form of strong convergence in $L^2(\Omega)$ and often some form of weak convergence of discrete gradients.

Obtaining such discrete $H_0^1$ estimates is not only the first step in proving the convergence of the scheme, but it is also crucial to ensure its numerical stability. Schemes for which such energy estimates can be established are called *coercive*. If a linear scheme is coercive and has a symmetric matrix, then it has a symmetric positive definite matrix and very efficient algorithms (Cholesky decomposition, conjugate gradient, etc.) can be used to compute its solution. Note however that the mere symmetry and positive-definiteness of the matrix are not enough to ensure the coercivity of the scheme, as this positive-definiteness must be uniform with respect to the mesh and must hold for a discrete $H_0^1$ norm satisfying (C2).

**Remark 1.3 (Consistency of Finite Volume methods).** In FV methods, the numerical fluxes $F_{K,\sigma}$ are consistent approximations of the exact fluxes $\overline{F}_{K,\sigma}$: if $F^\star_{K,\sigma}$ are the numerical fluxes computed by replacing the unknowns by the exact values of $\overline{u}$ and if all data are smooth, then

$$F^\star_{K,\sigma} = \overline{F}_{K,\sigma} + \mathcal{O}(|\sigma|\mathrm{diam}(K)) \tag{1.13}$$

(note that $\overline{F}_{K,\sigma} = \mathcal{O}(|\sigma|)$). It is however often said that FV methods do not provide consistent approximations of the operator $-\mathrm{div}(\Lambda\nabla\overline{u})$ "in the Finite Difference sense" (see Ref. 71, Chapter 2). We can indeed check that, in general,

$$\sum_{\sigma\in\mathcal{E}_K} F^\star_{K,\sigma} = \int_K -\mathrm{div}(\Lambda\nabla\overline{u}) + \mathcal{O}(|K|) \tag{1.14}$$

(note that $\int_K -\mathrm{div}(\Lambda\nabla\overline{u}) = \mathcal{O}(|K|)$). In fact, as often in mathematical analysis, everything is relative to topology. Relation (1.14) shows a non-consistency in $L^\infty$ or $L^2$ norm, but thanks to the flux consistency (1.13) and the conservativity of fluxes, we can prove that, for any $\varphi \in H_0^1(\Omega)$,

$$\sum_{K\in\mathcal{M}}\sum_{\sigma\in\mathcal{E}_K} F^\star_{K,\sigma}\varphi_K = -\int_\Omega \mathrm{div}(\Lambda\nabla\overline{u})(x)\varphi(x)\mathrm{d}x + \mathcal{O}(h_\mathcal{M}||(\varphi_K)_{K\in\mathcal{M}}||_{1,\mathrm{disc}}),$$

where $\varphi_K = \frac{1}{|K|}\int_K \varphi(x)\mathrm{d}x$ and $||\cdot||_{1,\mathrm{disc}}$ is the discrete $H_0^1$ norm of Sec. 2.1. Hence, $\sum_{\sigma\in\mathcal{E}_K} F^\star_{K,\sigma}$ is a consistent approximation of $\int_K -\mathrm{div}(\Lambda\nabla\overline{u})$ in some discrete dual $H_0^1$ norm and, because of this, establishing discrete $H_0^1$ estimates on approximate solutions is also crucial to pass to the limit in Step (C3).

**Remark 1.4 (Linearly exact scheme).** The consistency relation (1.13) is strongly related with the fact that the scheme is *linearly exact*, meaning that if the exact solution $\overline{u}$ to (1.1) is piecewise linear on the mesh then its interpolation is the solution to the scheme (i.e. the scheme exactly reproduces piecewise linear solutions). In this case, observed numerical orders of convergence([b]) are usually 2 for $\overline{u}$ and 1 for its gradient (at least for smooth solutions and linear schemes).

[b]Here and everywhere else in this paper, error estimates and orders of convergence are in some form of $L^2$ norm depending on the scheme.

### 1.3. *Maximum and minimum principles, or monotony*

A remarkable property of diffusion equations such as (1.1) is their maximum and minimum principles, see Ref. 94 or Chapter I in Ref. 120. In its strong form (also called the local minimum principle), the minimum principle states that, should $f$ be non-negative, the solution $\overline{u}$ to (1.1) cannot have a local minimum inside $\Omega$ unless it is constant. This prevents in particular the solution from presenting oscillating behaviours. This local minimum principle implies the following weaker (global) form

$$\text{if } f \geq 0 \text{ and } \overline{u}_b \geq 0 \text{ then } \overline{u} \geq 0, \tag{1.15}$$

as well as the (global) minimum-maximum principle (obtained by applying (1.15) to $\overline{u} - (\inf_{\partial\Omega} \overline{u}_b)$ and $(\sup_{\partial\Omega} \overline{u}_b) - \overline{u}$):

$$\text{if } f = 0 \text{ then } \inf_{\partial\Omega} \overline{u}_b \leq \overline{u} \leq \sup_{\partial\Omega} \overline{u}_b. \tag{1.16}$$

Assume that $U = ((u_i)_{i\in I}, (u_z)_{z\in B})$ is a vector gathering the unknowns $(u_i)_{i\in I}$ of the scheme and the discretised boundary conditions $(u_z)_{z\in B}$, computed from $\overline{u}_b$. If the scheme is written $S(U) = R$, where $R$ is a vector constructed from $f$, the discrete desirable versions of (1.15) and (1.16) are

$$\text{if } S(U) = R \geq 0 \text{ and } u_z \geq 0 \text{ for all } z \in B \text{ then } u_i \geq 0 \text{ for all } i \in I \tag{1.17}$$

(where $R \geq 0$ means that all components of $R$ are non-negative) and

$$\text{if } S(U) = 0 \text{ then } \inf_{z\in B} u_z \leq u_i \leq \sup_{z\in B} u_z \text{ for all } i \in I. \tag{1.18}$$

For linear schemes (i.e. $S$ is a linear function) that are exact on constant functions (i.e. $S(\mathbf{1}) = 0$, where $\mathbf{1}$ is the vector with all components equal to 1), the discrete minimum principle (1.17) implies the discrete minimum-maximum principle (1.18) (if $S(U) = 0$, apply (1.17) to $V = (\max_{z\in B} u_z)\mathbf{1} - U$ and $V = U - (\min_{z\in B} u_z)\mathbf{1}$, which both satisfy $V_b \geq 0$ for all $b \in B$ and $S(V) = 0$ by linearity of $S$). As we shall see in Sec. 6, non-linear schemes may satisfy (1.17) without satisfying (1.18).

The usual way in the literature to prove that a linear scheme satisfies (1.17) is to show that its matrix $A = (a_{ij})_{ij}$ is diagonally dominant by columns (i.e. $a_{ii} > 0$ for all $i$, $a_{ij} \leq 0$ for all $i \neq j$ and $a_{kk} \geq \sum_{i\neq k} |a_{ik}|$ for all $k$ with strict inequality for at least one $k$) and has a connected graph. Under these assumptions, it is easy to see that $A$ is invertible and that $A^{-1}$ only has non-negative coefficients ($A$ is thus an $M$-matrix), see Chapter 6 in Ref. 9. Provided that the scheme is written $S(U) = A(u_i)_{i\in I} - C(u_z)_{z\in B} = R$ where $C$ is a matrix with non-negative coefficients, we then obtain $(u_i)_{i\in I} = A^{-1}(R + C(u_z)_{z\in B}) \geq 0$ whenever $R \geq 0$ and $u_z \geq 0$ for all $z \in B$.

Satisfying a discrete minimum-maximum principle is particularly important in complex models such as multi-phase flows in reservoir engineering. Schemes that do not satisfy this principle may give rise to spurious oscillations which may lead to gas-oil numerical instabilities. Linear schemes for (1.1) satisfying (1.17) are also called *monotone*, as they preserve the order of boundary conditions (for non-negative right-hand sides) or of initial conditions (when applied to transient equations).

## 2. TPFA scheme

Let us assume that the medium is isotropic, i.e. $\Lambda(x) = \lambda(x)\mathrm{Id}$ for some scalar function $\lambda$. We also assume the following orthogonality conditions on the mesh:

$$\begin{array}{l} \forall\sigma \text{ edge between two control volumes } K, L \in \mathcal{M}\,,\ (\boldsymbol{x}_K\boldsymbol{x}_L)\perp\sigma\,, \\ \forall\sigma \in \mathcal{E}_{\text{ext}} \cap \mathcal{E}_K\,,\ \text{ the half-line } \boldsymbol{x}_K + [0,\infty)\mathbf{n}_{K,\sigma} \text{ intersects } \sigma. \end{array} \tag{2.1}$$

In Fig. 1, for example, this assumption is satisfied by the edge $\sigma$ between $K$ and $L$ but not by the edge between $K$ and $M$. Letting $\{\boldsymbol{x}_\sigma\} = (\boldsymbol{x}_K\boldsymbol{x}_L) \cap \sigma$ (or $\{\boldsymbol{x}_\sigma\} = (\boldsymbol{x}_K + [0,\infty)\mathbf{n}_{K,\sigma}) \cap \sigma$ if $\sigma \in \mathcal{E}_{\text{ext}}$), consistent approximations of the fluxes for small $h_{\mathcal{M}}$ are

$$\text{if } \sigma \in \mathcal{E}_K \cap \mathcal{E}_L : F_{K,\sigma} = \lambda_K|\sigma|\frac{u_K - u_\sigma}{\mathrm{d}(\boldsymbol{x}_K, \boldsymbol{x}_\sigma)} \text{ and } F_{L,\sigma} = \lambda_L|\sigma|\frac{u_L - u_\sigma}{\mathrm{d}(\boldsymbol{x}_L, \boldsymbol{x}_\sigma)}, \tag{2.2}$$

$$\text{if } \sigma \in \mathcal{E}_{\text{ext}} \cap \mathcal{E}_K : F_{K,\sigma} = \lambda_K|\sigma|\frac{u_K - u_\sigma}{\mathrm{d}(\boldsymbol{x}_K, \sigma)}, \tag{2.3}$$

where $\mathrm{d}(a,b) = |a-b|$, $\lambda_K$ is the value of $\lambda$ on $K$ and $u_\sigma$ approximates $\overline{u}(\boldsymbol{x}_\sigma)$. If $\sigma \in \mathcal{E}_{\text{ext}}$, $u_\sigma$ is fixed by $\overline{u}_b$([c]). If $\sigma \in \mathcal{E}_K \cap \mathcal{E}_L$, the additional unknown $u_\sigma$ is eliminated by imposing the conservativity (1.10) of fluxes and we get (see Ref. 71, Chapter 3):

$$F_{K,\sigma} = \tau_\sigma(u_K - u_L) \quad \text{with } \tau_\sigma = \frac{|\sigma|}{\mathrm{d}(\boldsymbol{x}_K, \boldsymbol{x}_L)}\frac{\lambda_K\lambda_L\mathrm{d}(\boldsymbol{x}_K, \boldsymbol{x}_L)}{\lambda_K\mathrm{d}(\boldsymbol{x}_L, \boldsymbol{x}_\sigma) + \lambda_L\mathrm{d}(\boldsymbol{x}_K, \boldsymbol{x}_\sigma)}. \tag{2.4}$$

The balance equation (1.9) of the discrete fluxes (2.3)-(2.4) then gives an FV scheme for (1.1) when $\Lambda = \lambda\mathrm{Id}$, called the Two Point Flux Approximation Finite Volume scheme (TPFA for short) since each flux is computed using only the 2 unknowns on each side of the edge.

**Remark 2.1.** As $\mathrm{d}(\boldsymbol{x}_K, \boldsymbol{x}_\sigma) + \mathrm{d}(\boldsymbol{x}_L, \boldsymbol{x}_\sigma) = \mathrm{d}(\boldsymbol{x}_K, \boldsymbol{x}_L)$, the transmissibility $\tau_\sigma$ involves an harmonic average of the values of $\Lambda$ in the cells on each side of $\sigma$. This harmonic average is well-known, in FV methods, to give a much more accurate solution than other averages.

**Remark 2.2.** If $\Lambda$ is an anisotropic full tensor, the same construction can be made (see Chapter 3 in Ref. 71) provided that the orthogonality condition (2.1) is replaced with (2.5), in which $D_{K,\sigma}$ is the straight line going through $\boldsymbol{x}_K$ and orthogonal to $\sigma$ for the scalar product induced by $\Lambda_K^{-1}$:

$$\begin{array}{l} \forall\sigma \text{ between two control volumes } K, L \in \mathcal{M}\,,\ D_{K,\sigma} \cap \sigma = D_{L,\sigma} \cap \sigma \neq \emptyset\,, \\ \forall\sigma \in \mathcal{E}_{\text{ext}} \cap \mathcal{E}_K\,,\ D_{K,\sigma} \cap \sigma \neq \emptyset. \end{array} \tag{2.5}$$

[c]Several choices are possible. If $\overline{u}_b$ is smooth enough, then one can take $u_\sigma = \overline{u}_b(\boldsymbol{x}_\sigma)$. Otherwise, $u_\sigma$ can be chosen as the average of $\overline{u}_b$ on $\sigma$.

### 2.1. *Coercivity*

Assume that $\overline{u}_b = 0$ and thus that $u_\sigma = 0$ for all $\sigma \in \mathcal{E}_{\rm ext}$. Multiplying the balance equation (1.9) by $u_K$, summing on $K \in \mathcal{M}$ and gathering by edges (=discrete integration by parts), we obtain, thanks to (2.4),

$$||u||_{1,\mathcal{D}}^2 := \sum_{\sigma\in\mathcal{E}_{\rm int}} \tau_\sigma (u_K - u_L)^2 + \sum_{\sigma\in\mathcal{E}_{\rm ext}} \tau_\sigma u_K^2 = \int_\Omega f(x)u(x)\mathrm{d}x \tag{2.6}$$

where $u$ is the piecewise constant function equal to $u_K$ on $K$ and, in the sums, $K$ and $L$ are the control volumes on each side of $\sigma \in \mathcal{E}_{\rm int}$ (we let $\tau_\sigma = \lambda_K \frac{|\sigma|}{\mathrm{d}(\boldsymbol{x}_K,\sigma)}$ whenever $\sigma \in \mathcal{E}_{\rm ext} \cap \mathcal{E}_K$). The left-hand side of (2.6) defines a discrete $H_0^1$ norm $||u||_{1,\rm disc}$ for which one can establish the discrete Poincaré inequality $||u||_{L^2(\Omega)} \leq \mathrm{diam}(\Omega)||u||_{1,\rm disc}$ and a discrete compactness result as in Step (C2) of Sec. 1.2, see Chapter 3 in Ref. 71. The TPFA scheme is thus coercive (with a symmetric matrix) and its convergence can be proved under the sole assumptions (1.2)–(1.4). Of course, error estimates can also be obtained if the data are more regular[86].

### 2.2. *Monotony*

Injecting (2.3)-(2.4) in the balance equation (1.9) we obtain, with the same conventions as in (2.6), for all $K \in \mathcal{M}$,

$$\sum_{\sigma\in\mathcal{E}_{\rm int}} \tau_\sigma (u_K - u_L) + \sum_{\sigma\in\mathcal{E}_{\rm ext}} \tau_\sigma u_K = \int_K f(x)\mathrm{d}x + \sum_{\sigma\in\mathcal{E}_{\rm ext}} \tau_\sigma u_\sigma. \tag{2.7}$$

From this expression we can see that the scheme's function (see Section 1.3) can be written $S(U) = A(u_K)_{K\in\mathcal{M}} - C(u_\sigma)_{\sigma\in\mathcal{E}_{\rm ext}}$, with $A$ diagonally dominant, symmetric and graph-connected, and all coefficients of $C$ non-negative. Sec. 1.3 then shows that the TPFA scheme is monotone.

**Remark 2.3.** Monotony of the TPFA scheme is in fact easy to prove from (2.7). If $f \geq 0$, $u_\sigma \geq 0$ for all $\sigma \in \mathcal{E}_{\rm ext}$ and $u_K = \min_{M\in\mathcal{M}} u_M < 0$ then the left-hand side of (2.7) is a non-negative sum of non-positive terms. Hence all terms are equal to 0 and $u_K = u_L$ for all neighbours $L$ of $K$. The minimal value $u_K$ thus propagates to all neighbours and, ultimately, to the whole connected domain. Using (2.7) for one boundary cell then contradicts the negativity of this minimal value.

In fact, this reasoning applied to $A^T$ gives a proof that the diagonal dominance by columns of $A$ and its graph connectedness entail the non-negativity of all coefficients of $A^{-1}$. It also shows that schemes with such matrices satisfy in fact a discrete version of the strong minimum principle: if $f \geq 0$, the solution to the scheme cannot have any interior minimum unless it is constant.

### 2.3. *The perfect scheme?*

The TPFA scheme is a cell-centred scheme (only involving cell unknowns), very cheap to implement and with a small stencil: 5 on 2D quadrilateral meshes and 7

on 3D hexahedral meshes. Its matrix is therefore very sparse and its solution easy to compute. For these reasons, it has been adopted in many engineering software, but it is not the perfect scheme...

Meshes available in field applications may be quite distorted and may have cells presenting various complex geometries, especially in basin simulation where alignment with geological layers and erosion may lead to hexahedra with collapsed faces. The orthogonality properties (2.1) or (2.5) are impossible to satisfy on these meshes and, should they fail for too many edges, the solution given by the TPFA scheme will be totally incorrect[1, 67, 80]. Other FV methods therefore had to be designed, providing consistent fluxes for general meshes and tensors.

## 3. MPFA methods

Consistent approximations of the fluxes $\overline{F}_{K,\sigma}$ on general meshes require the usage of more approximate values of $\overline{u}$ (in cells, on edges or at vertices) than the two at $\boldsymbol{x}_K$ and $\boldsymbol{x}_L$ on each side of $\sigma$. One easy way to get such values is to interpolate them from cell unknowns. This is the path chosen in Ref. 80 which introduces, for each edge, additional cell values located at points satisfying the orthogonality condition (2.5) for the considered edge, and then compute these values by convex combinations of existing cell unknowns. However, this scheme's construction and stability can only be ensured for grids not too distorted and tensors not too anisotropic.

Another idea is not to try and get back the orthogonality condition (2.5), but to use the additional values to compute approximate gradients, which in turn give approximate fluxes $F_{K,\sigma}$. However, the computation of the additional values must be done in a clever way, especially when $\Lambda$ is discontinuous, to ensure that the flux conservativity (1.10) is satisfied.

The Multi-Point Flux Approximation (MPFA) schemes are based on such a construction. Introduced in the mid- to late 90's[2–4, 59, 63], these methods assume that the solution is piecewise linear in some sub-cells around each vertex, introduce additional edge unknowns and express the linear variation of the solution to compute gradients and thus fluxes in these sub-cells. The edge unknowns are then eliminated (interpolated using cell unknowns) by writing *continuity equations* for the solution and *conservativity equations* for its fluxes. The final numerical fluxes are consistent, conservative and expressed only in terms of cell unknowns.

### 3.1. *O-method*

Several MPFA methods have been devised over the years and their main variation is on the choice of the local continuity and conservativity equations. Amongst those methods, the O-method (presented in Refs. 1, 3 for particular polygonal meshes) has received one of the largest coverage in literature on MPFA methods.

Let us first consider the 2D case. For each edge $\sigma$, we fix a point $\overline{\boldsymbol{x}}_\sigma$ on $\sigma$. Several choices are possible[3, 63] but we only consider here the case where $\overline{\boldsymbol{x}}_\sigma$ is the midpoint of $\sigma$. Then for each vertex $\boldsymbol{v}$ of the mesh, an *interaction region* is built by

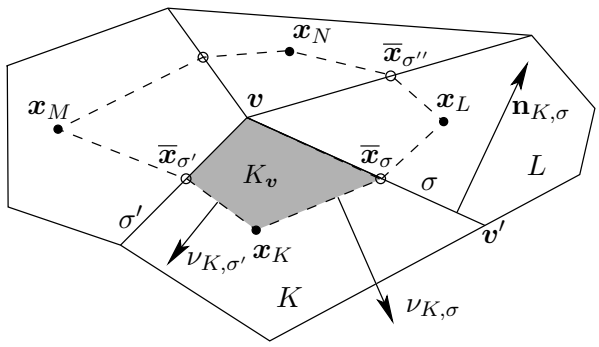


Fig. 2. Control volumes $(K, L, \ldots)$ and interaction region (enclosed in dotted line) for the MPFA O-method. $\nu_{K,\tau}$ = normal vector to $(\boldsymbol{x}_K\overline{\boldsymbol{x}}_\tau)$ with length $\mathrm{d}(\boldsymbol{x}_K, \overline{\boldsymbol{x}}_\tau)$ $(\tau = \sigma, \sigma')$.

joining the cell points $\boldsymbol{x}_K$ around $\boldsymbol{v}$ and the midpoints $\overline{\boldsymbol{x}}_\sigma$ of the edges containing $\boldsymbol{v}$ (see Fig. 2). This interaction region is made of one sub-cell $K_{\boldsymbol{v}}$ per cell $K$ and the solution $\overline{u}$ is approximated by a function that is linear inside each sub-cell around $\boldsymbol{v}$ ([d]).

At this stage, *continuity of this piecewise linear approximation is assumed at each edge midpoint* $\overline{\boldsymbol{x}}_\sigma$ around $\boldsymbol{v}$. We can therefore talk about the value $u_\sigma$ of this function at $\overline{\boldsymbol{x}}_\sigma$, and its constant gradient $\nabla_{K_{\boldsymbol{v}}} u$ on $K_{\boldsymbol{v}}$ satisfies

$$\nabla_{K_{\boldsymbol{v}}} u \cdot (\boldsymbol{x}_K - \overline{\boldsymbol{x}}_\tau) = u_K - u_\tau \quad (\tau = \sigma \text{ or } \sigma'). \tag{3.1}$$

Assuming that the vectors $\overrightarrow{\boldsymbol{x}_K\overline{\boldsymbol{x}}_\sigma}$ and $\overrightarrow{\boldsymbol{x}_K\overline{\boldsymbol{x}}_{\sigma'}}$ are linearly independent, these two projections of $\nabla_{K_{\boldsymbol{v}}} u$ on these vectors provide[3] the whole gradient $\nabla_{K_{\boldsymbol{v}}} u$:

$$\nabla_{K_{\boldsymbol{v}}} u = -\frac{1}{2T}\left((u_\sigma - u_K)\nu_{K,\sigma'} + (u_{\sigma'} - u_K)\nu_{K,\sigma}\right) \tag{3.2}$$

where $T$ is the area of triangle $(\boldsymbol{x}_K\overline{\boldsymbol{x}}_\sigma\overline{\boldsymbol{x}}_{\sigma'})$ and $\nu_{K,\tau}$ $(\tau = \sigma \text{ or } \sigma')$ is the normal to $(\boldsymbol{x}_K\overline{\boldsymbol{x}}_\tau)$, pointing outward this triangle and having length $\mathrm{d}(\boldsymbol{x}_K, \overline{\boldsymbol{x}}_\tau)$.

Sub-fluxes across the half-edges $[\boldsymbol{v}\overline{\boldsymbol{x}}_\tau]$ around $\boldsymbol{v}$ are then computed using these gradients, and therefore depend on the cell unknowns $u_K, u_L, \ldots$ and the edge unknowns $u_\sigma, u_{\sigma'}, \ldots$ around $\boldsymbol{v}$. For example, the sub-flux from $K$ through $[\boldsymbol{v}\overline{\boldsymbol{x}}_\tau]$ is

$$F_{K,\tau,\boldsymbol{v}} = -\mathrm{d}(\boldsymbol{v}, \overline{\boldsymbol{x}}_\tau)\Lambda_K \nabla_{K_{\boldsymbol{v}}} u \cdot \mathbf{n}_{K,\tau} \quad (\tau = \sigma \text{ or } \sigma'). \tag{3.3}$$

The next step is to eliminate the edge unknowns involved in these sub-fluxes. This is done by imposing the conservativity of the fluxes around $\boldsymbol{v}$:

$$\begin{aligned}&\text{For any edge } \tau \text{ containing } \boldsymbol{v}, \text{ if } R, S \text{ are the cells on each side of } \tau,\\ &F_{R,\tau,\boldsymbol{v}} + F_{S,\tau,\boldsymbol{v}} = 0.\end{aligned} \tag{3.4}$$

[d]This linear approximation is natural if the mesh size is small enough since, usually, $\Lambda$ and $f$ are assumed to be constant or smooth in $K$, so that $\overline{u}$ is expected to be smooth inside $K$.

Note that if $\tau$ is an edge on $\partial\Omega$, $u_\tau$ is not eliminated but fixed by the value of $\overline{u}_b$ (Neumann boundary conditions are also easily handled, either by imposing the value of $F_{K,\tau,\boldsymbol{v}}$ whenever $\tau$ is a boundary edge or by using – which is equivalent – ghosts cells outside $\Omega$[1, 3]).

From the construction (3.2)-(3.3) of the sub-fluxes, (3.4) gives a linear square system on the edge unknowns $u_\sigma, u_{\sigma'}, \ldots$ around $\boldsymbol{v}$ which is, in general, invertible and gives an expression of these edge unknowns in terms of the cell unknowns $u_K, u_L, \ldots$ around $\boldsymbol{v}$. Plugged into (3.2)-(3.3), these expressions of the edge unknowns give formulas for the sub-flux $F_{K,\sigma,\boldsymbol{v}}$ using only the cell unknowns $u_K, u_L, \ldots$ around $\boldsymbol{v}$. The same procedure performed from the other vertex $\boldsymbol{v}'$ of $\sigma$ gives a second sub-flux $F_{K,\sigma,\boldsymbol{v}'}$. The global flux through $\sigma$, that is $F_{K,\sigma} = F_{K,\sigma,\boldsymbol{v}} + F_{K,\sigma,\boldsymbol{v}'}$, is therefore a function of all the unknowns $u_K, u_L, \ldots$ in all the cells around $\boldsymbol{v}$ and $\boldsymbol{v}'$. By construction, $(F_{K,\sigma})_{K\in\mathcal{M},\,\sigma\in\mathcal{E}_K}$ naturally satisfy the conservativity equation (1.10) and the O-scheme is thus obtained by only imposing the balance equation (1.9).

**Remark 3.1 (Two edge unknowns per edge).** The elimination of the edge unknowns is performed locally around each vertex $\boldsymbol{v}$ and the continuity at the edge midpoints is only enforced when eliminating the edge unknowns around $\boldsymbol{v}$. The edge unknown $u_\sigma$ at $\overline{\boldsymbol{x}}_\sigma$ when viewed from vertex $\boldsymbol{v}$ therefore may be different from the edge unknown at $\overline{\boldsymbol{x}}_\sigma$ viewed from the other vertex $\boldsymbol{v}'$ of $\sigma$. This may look strange, as there is no particular reason for $\overline{u}$ to have different values at $\overline{\boldsymbol{x}}_\sigma$, but this comes from the construction of the MPFA method which cannot assume that the linear variations of $\overline{u}$ in $K_{\boldsymbol{v}}$ and in $K_{\boldsymbol{v}'}$ have the same value at $\overline{\boldsymbol{x}}_\sigma$ (otherwise, some flux conservativity equations could not be satisfied).

The generalisation of this construction to 3D polyhedral cells is pretty straightforward[5] if we assume that

$$\text{for each cell } K \text{ and each vertex } \boldsymbol{v} \text{ of } K\text{, exactly 3 faces of } K \text{ meet at } \boldsymbol{v}. \tag{3.5}$$

In this case, the sub-cell $K_{\boldsymbol{v}}$ is the hexahedron obtained by joining $\boldsymbol{v}$, $\boldsymbol{x}_K$, the midpoints of edges of $K$ having $\boldsymbol{v}$ as vertex and the three centres of gravity $\overline{\boldsymbol{x}}_\sigma$, $\overline{\boldsymbol{x}}_{\sigma'}$ and $\overline{\boldsymbol{x}}_{\sigma''}$ of the faces of $K$ meeting at $\boldsymbol{v}$. Three temporary unknowns $u_\sigma$, $u_{\sigma'}$ and $u_{\sigma''}$ are introduced at the centres of gravity of the faces and, assuming that the vectors $\overrightarrow{\boldsymbol{x}_K\overline{\boldsymbol{x}}_\sigma}$, $\overrightarrow{\boldsymbol{x}_K\overline{\boldsymbol{x}}_{\sigma'}}$ and $\overrightarrow{\boldsymbol{x}_K\overline{\boldsymbol{x}}_{\sigma''}}$ are linearly independent, the three equations (3.1) for $\tau = \sigma$, $\sigma'$ and $\sigma''$ can be solved for $\nabla_{K_{\boldsymbol{v}}} u$, which is thus computed in terms of $u_K, u_\sigma, u_{\sigma'}$ and $u_{\sigma''}$. The rest of the construction follows as in 2D, the edge unknowns being eliminated thanks to the sub-fluxes conservativity.

**Remark 3.2.** This procedure even allows for non-planar faces (which often occurs in hexahedral meshes in 3D, as the four vertices of a given face may not be on the same plane), provided that the vectors $\mathbf{n}_{K,\sigma}$ are defined as the mean value on $\sigma$ of the pointwise normal vector to the face[1, 5].

Construction of an MPFA O-method on 3D meshes is much less obvious when (3.5) does not hold. In this case, for some vertices $\boldsymbol{v}$ the system (3.1) has 4 or

more equations and, since (in general) the gradient $\nabla_{K_{\boldsymbol{v}}} u$ is entirely determined by $u_K$ and only 3 face unknowns, the other face unknowns will be fixed by those 3 face unknowns. No degrees of freedom then remain to impose the conservativity of the corresponding sub-fluxes. Ref. 12 however introduces a scheme on general polygonal or polyhedral meshes (without assuming (3.5)), which coincides with the MPFA O-method in 2D and in 3D when (3.5) holds. This reference also presents a new formulation of the O-method, based on a discrete form of the variational formulation (1.5) rather than on a flux balance (1.9).

**Remark 3.3.** Explicit formulas for the fluxes in terms of the cell unknowns can be obtained[1] in the case of parallelogram or parallelepiped meshes and $\Lambda$ constant. In other cases, System (3.4) has to be numerically solved.

**Remark 3.4.** For non-conforming meshes such as the ones appearing in reservoirs with faults, this MPFA O-method leads to unacceptable fluxes and must therefore be modified[8], by introducing two linear approximations of $\overline{u}$ in some sub-cells $K_{\boldsymbol{v}}$.

### 3.2. *L- and G-methods*

As already mentioned, many choices are available to compute consistent conservative fluxes from piecewise linear approximations of $\overline{u}$ around each vertex. Another well-studied MPFA method is the L-method, introduced in Ref. 7 for quadrilateral meshes. The major difference of the L-method with respect to the O-method are: (i) no edge unknowns need to be introduced as the gradient themselves are the additional unknowns to eliminate, (ii) the continuity and sub-flux conservativity equations are written only on 2 edges, (iii) the continuity of the piecewise linear approximation is imposed on whole edges (not only at edge midpoints), and (iv) the gradients and piecewise linear approximation constructed on sub-cells $K_{\boldsymbol{v}}$, $L_{\boldsymbol{v}}$, ..., depend on the edge $\sigma$ through which we want to compute the flux and are thus not common to all sub-fluxes around $\boldsymbol{v}$.

Still using the notations in Fig. 2, let us consider the sub-flux $F_{K,\sigma,\boldsymbol{v}}$ and let us introduce $\nabla^{\sigma}_{M_{\boldsymbol{v}}} u$, $\nabla^{\sigma}_{K_{\boldsymbol{v}}} u$ and $\nabla^{\sigma}_{L_{\boldsymbol{v}}} u$, the three constant gradients of a piecewise linear approximation of $\overline{u}$ on $M_{\boldsymbol{v}} \cup K_{\boldsymbol{v}} \cup L_{\boldsymbol{v}}$. As mentioned above, these gradients will only be used to compute $F_{K,\sigma,\boldsymbol{v}}$ and other gradients would be used if we were to compute $F_{K,\sigma',\boldsymbol{v}}$ for example (ergo the super-script $\sigma$ in $\nabla^{\sigma}_{M_{\boldsymbol{v}}} u$, $\nabla^{\sigma}_{K_{\boldsymbol{v}}} u$, $\nabla^{\sigma}_{L_{\boldsymbol{v}}} u$). In the L-method, full continuity is imposed for this approximation:

$$\begin{aligned} &\forall x \in [\boldsymbol{v}\overline{\boldsymbol{x}}_{\sigma'}] \,:\, u_K + (\nabla^{\sigma}_{K_{\boldsymbol{v}}} u)\cdot(x - \boldsymbol{x}_K) = u_M + (\nabla^{\sigma}_{M_{\boldsymbol{v}}} u)\cdot(x - \boldsymbol{x}_M) \\ &\forall x \in [\boldsymbol{v}\overline{\boldsymbol{x}}_{\sigma}] \,:\, u_K + (\nabla^{\sigma}_{K_{\boldsymbol{v}}} u)\cdot(x - \boldsymbol{x}_K) = u_L + (\nabla^{\sigma}_{L_{\boldsymbol{v}}} u)\cdot(x - \boldsymbol{x}_L) \end{aligned} \tag{3.6}$$

These equations can be equivalently written only at $\boldsymbol{v}$, $\overline{\boldsymbol{x}}_{\sigma'}$ and $\boldsymbol{v}$, $\overline{\boldsymbol{x}}_{\sigma}$ respectively, and they provide 4 conditions on the 6 degrees of freedom of the 3 gradients. The sub-flux conservativities give the remaining 2 equations

$$\begin{aligned} &\Lambda_K \nabla^{\sigma}_{K_{\boldsymbol{v}}} u \cdot \mathbf{n}_{K,\sigma'} + \Lambda_M \nabla^{\sigma}_{M_{\boldsymbol{v}}} u \cdot \mathbf{n}_{M,\sigma'} = 0 \\ &\Lambda_K \nabla^{\sigma}_{K_{\boldsymbol{v}}} u \cdot \mathbf{n}_{K,\sigma} + \Lambda_L \nabla^{\sigma}_{L_{\boldsymbol{v}}} u \cdot \mathbf{n}_{L,\sigma} = 0. \end{aligned} \tag{3.7}$$

System (3.6)-(3.7) is therefore square and invertible in general (otherwise, work-arounds can be designed[10]). The local gradients can then be expressed in terms of the cell unknowns $u_M$, $u_K$ and $u_L$, and so does the sub-flux $F_{K,\sigma,\boldsymbol{v}} = -\mathrm{d}(\boldsymbol{v}, \overline{\boldsymbol{x}}_\sigma)\Lambda_K \nabla^\sigma_{K_{\boldsymbol{v}}} u \cdot \mathbf{n}_{K,\sigma}$.

**Remark 3.5.** If $\sigma$ or $\sigma'$ is a boundary edge, then the corresponding right-hand side in (3.6) is fixed by the value of $\overline{u}_b$ and the corresponding conservativity equation in (3.7) is removed. System (3.6)-(3.7) remains square, of size 4 (if only one edge is a boundary edge) or 2 (if both $\sigma$ and $\sigma'$ are boundary edges).

This is however but one choice that can be made to compute the flux through $\sigma$. Another natural choice would be to use the edges $\sigma$ and $\sigma''$ instead of $\sigma$ and $\sigma'$ in (3.6)-(3.7). This would give another sub-flux $F_{K,\sigma,\boldsymbol{v}}$ in terms of $u_K$, $u_L$, $u_N$. In the L-method, the choice between using $\sigma, \sigma'$ or $\sigma, \sigma''$ is made according to a criterion[7] involving transmissibility signs and ensuring that each cell unknown $u_M, u_K, u_L$ or $u_K, u_L, u_N$ contributes with the most physically-relevant sign to the sub-flux through $[\boldsymbol{v}\overline{\boldsymbol{x}}_\sigma]$. Full formulas can be obtained[7] in the case of homogeneous media and grids made of parallelograms and, in the case of moderate skewness of the diffusion tensor and the grid, the chosen criterion indeed leads to the correct signs.

**Remark 3.6.** The L-method does not suffer from the same issues (and does not need modification) as the original MPFA O-method on meshes with faults[7].

A generalisation of the L-method, the G-method, has been proposed in Ref. 10. Its principles are the same (full continuity of $\overline{u}$ and conservativity of the fluxes on some edges), but the above selection criterion is not applied and the global fluxes through $\sigma$ are built as convex combinations of all possible sub-fluxes through this edge. These combinations are chosen according to some local index, designed to improve the coercivity properties of the scheme.

**Remark 3.7.** Contrary to the O-scheme, construction of the L- and G-scheme on general 3D polyhedral meshes is straightforward[10]. Indeed, no face unknown is introduced and there is always, whatever the number of faces that meet at a given vertex, enough degrees of freedom (one local constant gradient per face which contains the vertex) to impose the local conservativity of sub-fluxes.

**Remark 3.8.** The MPFA U-method[3] is based on principles a bit similar to the L-method, computing the flux through $[\boldsymbol{v}\overline{\boldsymbol{x}}_\sigma]$ by mixing midpoint continuity (3.1) (at $\overline{\boldsymbol{x}}_\sigma$) and the full continuity on $[\boldsymbol{v}\overline{\boldsymbol{x}}_{\sigma'}]$ and $[\boldsymbol{v}\overline{\boldsymbol{x}}_{\sigma''}]$ (as in (3.6)). The local gradients also depend on the edge $\sigma$ through which we compute the sub-flux.

### 3.3. *Coercivity and convergence of MPFA methods*

MPFA methods are linearly exact, and therefore consistent in the sense (1.13), but they are not coercive in general. Using reference elements (or curvilinear coordinates) such as in Finite Element methods, constructions of symmetric definite

positive MPFA O-methods have been proposed on quadrilateral (hexahedral in 3D) meshes in Refs. 1, 6, 62 and on general 2D polygonal meshes in Ref. 83. However, these methods method turn out to be numerically less stable than the MPFA O-method presented above[6] (constructed in physical space). Convergence of these reference element-based O-methods even sometimes seems to be lost in presence of anisotropy or perturbed mesh, when the O-method constructed in physical space still converges[5, 6, 99]. A reason for this loss of convergence, in view of Sec. 1.2, is probably the following[6]: when constructing the method on a reference mesh, the coercivity properties of the scheme matrix depends on the mesh regularity (via the Piola mapping) and may degenerate for strongly perturbed meshes as the mesh size tends to 0, thus preventing from establishing energy estimates in a proper discrete $H_0^1$ norm for which the compactness result of Step (C2) in Sec. 1.2 would hold.

It has been proved that the physical O-method is coercive (and gives a symmetric definite positive matrix) on meshes made of parallelograms (parallelepiped in 3D) with $(\boldsymbol{x}_K)_{K\in\mathcal{M}}$ the centres of gravity of the cells[5, 12]. This is also true for meshes made of triangles (tetrahedra in 3D), provided that the unknown $u_\sigma$ used to construct the piecewise linear approximation of $\overline{u}$ in $K_{\boldsymbol{v}}$ is not located at $\overline{\boldsymbol{x}}_\sigma$ but closer to $\boldsymbol{v}$ (see Refs. 12, 102). Except in those particular instances, proofs of convergence of MPFA methods are always done by *assuming* some coercivity property.

Ref. 99 compares the MPFA O-method on 2D quadrilateral meshes to a non-symmetric Mixed Finite Element method (using a particular quadrature rule) and obtains, under a global coercivity assumption on the system matrix, $\mathcal{O}(h_{\mathcal{M}})$ error estimates for the approximate solution and fluxes, under the assumptions $\Lambda \in C^1(\overline{\Omega})$ and $\overline{u} \in H^2(\Omega)$. In a recent study[98], the MPFA O-method is compared on 2D or 3D polyhedral meshes satisfying (3.5) to a non-symmetric Mimetic Finite Difference method (see Sec. 4). Under local coercivity assumptions, $\mathcal{O}(h_{\mathcal{M}}^\alpha)$ error estimates are obtained when $\Lambda \in C^1(\overline{\Omega})$ and $\overline{u} \in H^{1+\alpha}(\Omega)$ ($\alpha > 1/2$ in 3D).

The regularity assumptions on $\Lambda$ and $\overline{u}$ required to establish these error estimates are not compatible with usual field applications (see Sec. 1.2). It is however possible to perform the full convergence analysis of the MPFA O- and L-method without assuming any non-physical smoothness on the data, by following the path sketched in Sec. 1.2. This is done in Ref. 12 for the MPFA O-method and in Ref. 10 for the MPFA L- and G-method. In these references, the convergence of MPFA methods on generic grids, in 2D or 3D (without assuming (3.5)), is proved by only assuming (1.2)—(1.4) and some local coercivity conditions which can be checked in numerical experiments.

The numerical study of the convergence of MPFA methods has also been performed in a number of articles[5, 67, 125]. As expected, the numerical orders of convergence of the O-method are usually $\mathcal{O}(h_{\mathcal{M}}^2)$ for $\overline{u}$ and $\mathcal{O}(h_{\mathcal{M}})$ for the fluxes, provided that $\overline{u} \in H^2$. If $\overline{u} \in H^{1+\alpha}$ with $\alpha \geq 0$, the orders of convergence seem to be[5] $\min(2, 2\alpha)$ for $\overline{u}$ and $\min(1, \alpha)$ for its fluxes ($\min(2, \alpha)$ for the fluxes in case of

smooth meshes). It has nonetheless been noticed[12] that, for anisotropy ratios (the largest eigenvalue of $\Lambda$ divided by the smallest eigenvalue of $\Lambda$) of order 1000 or more, the MPFA O-method no longer seems to converge on distorted grids, due to its loss of coercivity.

L- and G-methods have similar numerical behaviours, but they seem more stable than the O-method in presence of strong anisotropy or on irregular meshes used in basin simulation[7, 10].

### 3.4. *Maximum principle for MPFA methods*

When the mesh satisfies the orthogonality condition (2.5), MPFA methods are identical to the TPFA scheme and are therefore monotone. As mentioned, however, such orthogonality conditions are too restrictive in practice.

For some particular meshes, such as polygonal meshes whose cells are the union of triangles satisfying the Delaunay condition (the interaction regions are then triangles), the O-method is monotone if $\Lambda$ is constant. In the general case, conditions can be found[66] on the triangle angles and the diffusion tensor to ensure that the O-method gives rise to an M-matrix, and these conditions can be used to modify the positions of the mesh vertices in order to try and get an M-matrix. However, for large anisotropy ratios, such a modification may fail.

In most cases, the L-method displays better monotony properties than the O-method. The sufficient conditions of Ref. 123 (see below) are satisfied by the L-method on a larger class of meshes and tensors than for the O-method and, even in cases where monotony is violated, the L-method seems to present much less oscillations than the O-method[7].

One way to mitigate the problem of large anisotropy in the O-method, which leads to non-monotony and inaccuracies, is to apply a stretching[4] of the physical space to reduce the anisotropy ratio of $\Lambda$. This stretching does not seem necessary for regular hexagonal meshes but mandatory for triangular meshes when the anisotropy ratio is larger than 10.

The inaccuracy of the O-method in case of strong anisotropy can also be reduced by using a variant of the MPFA O-method introduced (in 2D) separately in Ref. 37 under the name "Enriched MPFA O-method" (EMPFA) and in Ref. 60 under the name "Full pressure support scheme" (FPS). This method relaxes the constraints on edge and cell unknowns by adding vertices unknowns, which gives enough degrees of freedom to assume the full continuity of the approximation of $\overline{u}$ on the sub-edges (not only at midpoints). This approximation is taken either piecewise linear (on the triangles $\overline{\boldsymbol{x}}_\sigma \boldsymbol{v} \boldsymbol{x}_K$, $\boldsymbol{x}_K \boldsymbol{v} \overline{\boldsymbol{x}}_{\sigma'}$, etc.) or piecewise bilinear (on the subcells $\boldsymbol{v}\overline{\boldsymbol{x}}_{\sigma'}\boldsymbol{x}_K\overline{\boldsymbol{x}}_\sigma$, $\boldsymbol{v}\overline{\boldsymbol{x}}_\sigma\boldsymbol{x}_L\overline{\boldsymbol{x}}_{\sigma''}$, etc.) and the new vertex unknown at $\boldsymbol{v}$ is eliminated by integrating (1.1) on a small domain around $\boldsymbol{v}$. The monotony (using M-matrix conditions introduced Ref. 63) and coercivity of the bilinear variant are analysed for quadrangular meshes in Ref. 60 and for triangular meshes in Ref. 82. However, even if the EMPFA/FPS method improves the monotony properties of the O-method in

a number of numerical tests, it remains unstable (non coercive) in case of strong anisotropy[128]. According to Ref. 60, 82, these improved monotony properties stem from imposing the continuity of the approximation on whole sub-edges, which prevents the EMPFA/FPS method from displaying decoupling properties of the O-method shown to be the cause of spurious oscillations. As mentioned above, the L-method also imposes continuities of full edges and presents improved monotony characteristics with respect to the O-method (its extension to 3D meshes moreover appears to be more straightforward than the extension of cell-centred EMPFA/FPS method). However, to our best knowledge, numerical or theoretical comparisons of the EMPFA/FPS and L methods still remain to be done.

A series of interesting results deserves to be mentioned here on the issue of the monotony of generic 9-point schemes on quadrilateral grids (which contain the MPFA methods). Sufficient conditions[122, 123] for the monotony of such scheme can be obtained if $\Lambda$ is constant, which provide guidance to generate meshes on which MPFA methods are monotone, and also show that 7-point methods (such as the L-method) enjoy better monotony properties in general[7]. These results also prove[96] that no linear 9-point scheme on generic quadrilateral meshes, which is exact on linear solutions, can be monotone for any $\Lambda$ (this has already been noticed, under another form, in Ref. 97).

### 3.5. *To summarise: MPFA methods*

The main strengths of MPFA methods are their cell-centred characteristic and a local computation of the fluxes (only cell unknowns close to an edge are used in the computation of the flux across this edge), which lead to acceptable stencils: 9 on 2D quadrilaterals, 27 on 3D hexahedral. A (small) disadvantage is the necessity to solve local systems to eliminate the edge/gradient unknowns, which may prove non-invertible in some cases and therefore require to locally modify the method[10, 129]. This however seems to happen relatively rarely and most numerical tests presented in the literature run without this issue.

A more undesirable characteristic of the MPFA method is their *conditional* coercivity and monotony. Despite numerous works on the topic, it is not always obvious to establish *a priori* the range of coercivity or monotony of an MPFA method on a generic mesh or with a generic diffusion tensor. As a consequence, unforeseen instabilities and loss of convergence may occur.

The question therefore remains to find a FV method which would be unconditionally coercive and monotone on any type of mesh...

## 4. HMM methods

Hybrid Mimetic Mixed (HMM) methods are made up of three families of methods, separately developed in the last ten years or so: the Hybrid Finite Volume method[74] (HFV), the Mimetic Finite Difference method[25, 28] (MFD) and the Mixed Finite Volume method[52] (MFV). It has recently been understood[54] that all these methods

are in fact identical and, therefore, that any analysis made for one also applies to the other two.

In HMM methods, the main unknowns are cell unknowns $(u_K)_{K\in\mathcal{M}}$ and edge unknowns $(u_\sigma)_{\sigma\in\mathcal{E}}$ (approximations of $(\overline{u}(\overline{\boldsymbol{x}}_\sigma))_{\sigma\in\mathcal{E}}$ where, as in Sec. 3, $\overline{\boldsymbol{x}}_\sigma$ is the centre of gravity of $\sigma$). Of the three families gathered in HMM methods, MFV methods are the ones with the most classical FV presentation, involving imposed balance and conservativity equations (1.9)-(1.10). Contrary to MPFA methods, edge unknowns are not eliminated and the computation of the fluxes is made through local inner products, thus ensuring the coercivity of the scheme.

For given fluxes $F_K = (F_{K,\sigma})_{\sigma\in\mathcal{E}_K}$ on $\partial K$, we introduce the vector

$$\mathbf{v}_K(F_K) = -\frac{1}{|K|}\Lambda_K^{-1}\sum_{\sigma\in\mathcal{E}_K} F_{K,\sigma}(\overline{\boldsymbol{x}}_\sigma - \boldsymbol{x}_K). \tag{4.1}$$

Stokes' formula shows that if $\overline{u}$ is linear in $K$ and $F_{K,\sigma} = -|\sigma|\Lambda_K\nabla\overline{u}_{|K}\cdot\mathbf{n}_{K,\sigma}$, then $\mathbf{v}_K(F_K) = \nabla\overline{u}_{|K}$. Hence, $\mathbf{v}_K(F_K)$ can be considered as a consistent approximation of $\nabla\overline{u}$ on $K$. Letting

$$T_K(F_K) = (T_{K,\sigma}(F_K))_{\sigma\in\mathcal{E}_K} \text{ with } T_{K,\sigma}(F_K) = \frac{1}{|\sigma|}F_{K,\sigma} + \Lambda_K\mathbf{v}_K(F_K)\cdot\mathbf{n}_{K,\sigma}, \tag{4.2}$$

the following local inner product is defined

$$[F_K, G_K]_K = |K|\mathbf{v}_K(F_K)\cdot\Lambda_K\mathbf{v}_K(G_K) + T_K(G_K)^T\mathbb{B}_K T_K(F_K) \tag{4.3}$$

(where $\mathbb{B}_K$ is a symmetric definite positive matrix) and the relation between the fluxes and the cell and edge unknowns is

$$\forall G_K = (G_{K,\sigma})_{\sigma\in\mathcal{E}_K}\in\mathbb{R}^{\mathcal{E}_K} \;:\; [F_K, G_K]_K = \sum_{\sigma\in\mathcal{E}_K}(u_K - u_\sigma)G_{K,\sigma}. \tag{4.4}$$

An MFV scheme is defined by (1.9)-(1.10)-(4.2)-(4.3)-(4.4) for some choices of $(\mathbb{B}_K)_{K\in\mathcal{M}}$, with Dirichlet boundary conditions enforced by imposing the value of $u_\sigma$ if $\sigma\in\mathcal{E}_{\text{ext}}$. Neumann boundary conditions are as easily considered[34] by imposing the value of $F_{K,\sigma}$ for all $\sigma\in\mathcal{E}_{\text{ext}}$.

**Remark 4.1.** For a given edge $\sigma\in\mathcal{E}_K$, using $G_K(\sigma) = (\delta_{\sigma,\sigma'})_{\sigma'\in\mathcal{E}_K}$ ($\delta_{\sigma,\sigma'}$ being Kronecker's symbol), we can see[54] that

$$u_\sigma - u_K = \mathbf{v}_K(F_K)\cdot(\overline{\boldsymbol{x}}_\sigma - \boldsymbol{x}_K) - T_K(G_K(\sigma))^T\mathbb{B}_K T_K(F_K). \tag{4.5}$$

Given that $T_K$ vanishes on exact fluxes of linear functions and that $\mathbf{v}_K(F_K)\approx\nabla\overline{u}_{|K}$, (4.5) shows that (4.4) is a Taylor expansion with second order remainder.

MFD methods are constructed starting from (4.4) and looking for inner products $[\cdot,\cdot]_K$ which satisfy the following consistency condition (discrete Stokes' formula): for all affine function $q$ and all $G_K = (G_{K,\sigma})_{\sigma\in\mathcal{E}_K}\in\mathbb{R}^{\mathcal{E}_K}$,

$$[(\Lambda\nabla q)^I, G]_K + \int_K q(x)(\mathcal{DIV}^h G_K)\mathrm{d}x = \sum_{\sigma\in\mathcal{E}_K}\frac{1}{|\sigma|}G_{K,\sigma}\int_\sigma q(x)\mathrm{d}S(x), \tag{4.6}$$

where $((\Lambda\nabla q)^I)_{K,\sigma} = |\sigma|\Lambda_K\nabla q_{|K}\cdot\mathbf{n}_{K,\sigma}$ and $\mathcal{DIV}^h G_K = \frac{1}{|K|}\sum_{\sigma\in\mathcal{E}_K} G_{K,\sigma}$ is the natural discrete divergence of the discrete vector field $G_K$. From the consistency condition (4.6), an algebraic decomposition of the matrix of $[\cdot,\cdot]_K$([e]) can be obtained[28] and used to prove[54] that any inner product satisfying (4.6) has the form (4.3) for some symmetric positive definite $\mathbb{B}_K$.

Relation (4.4) can be inverted to express the fluxes in terms of the cell and edge unknowns and eliminate them. By doing so, we obtain[54] the HFV scheme. To write down this formulation of the HMM methods, we introduce for any given vector $u = ((u_K)_{K\in\mathcal{M}}, (u_\sigma)_{\sigma\in\mathcal{E}})$ the following discrete gradient in $K$:

$$\nabla_K u = \frac{1}{|K|}\sum_{\sigma\in\mathcal{E}_K} |\sigma|(u_\sigma - u_K)\mathbf{n}_{K,\sigma}. \tag{4.7}$$

Stokes' formula shows that this gradient is exact if the vector $u$ interpolates a linear function at $(\boldsymbol{x}_K)_{K\in\mathcal{M}}$, $(\overline{\boldsymbol{x}}_\sigma)_{\sigma\in\mathcal{E}}$ (it can also be seen[54] that if $u$ and $F_K$ are related by (4.4) then $\nabla_K u = \mathbf{v}_K(F_K)$). The function

$$S_K(u) = (S_{K,\sigma}(u))_{\sigma\in\mathcal{E}_K} \text{ with } S_{K,\sigma}(u) = u_\sigma - u_K - \nabla_K u\cdot(\overline{\boldsymbol{x}}_\sigma - \boldsymbol{x}_K) \tag{4.8}$$

is therefore a first order Taylor expansion, which vanishes on interpolants of linear functions. The formulation of the HFV method is then: find $u = ((u_K)_{K\in\mathcal{M}}, (u_\sigma)_{\sigma\in\mathcal{E}})$ (where $u_\sigma$ is fixed by $\overline{u}_b$ if $\sigma\in\mathcal{E}_{\rm ext}$) such that, for any vector $v = ((v_K)_{K\in\mathcal{M}}, (v_\sigma)_{\sigma\in\mathcal{E}})$ with $v_\sigma = 0$ if $\sigma\in\mathcal{E}_{\rm ext}$,

$$\sum_{K\in\mathcal{M}} |K|\Lambda_K\nabla_K u\cdot\nabla_K v + \sum_{K\in\mathcal{M}} S_K(v)^T\widetilde{\mathbb{B}}_K S_K(u) = \sum_{K\in\mathcal{M}} v_K\int_K f, \tag{4.9}$$

where $(\widetilde{\mathbb{B}}_K)_{K\in\mathcal{M}}$ are symmetric positive definite matrices (which depend on the matrices $(\mathbb{B}_K)_{K\in\mathcal{M}}$ in (4.4)). This formulation is clearly a discretisation of the weak formulation (1.5) of (1.1).

**Remark 4.2.** The original MFV, MFD and HFV methods are slightly less general than the ones presented here. The original MFV method writes (4.5) with a different (stronger) stabilisation, the original MFD method only consider the case where $\boldsymbol{x}_K$ is the centre of gravity of $K$, and the original HFV method is only written using diagonal matrices $\widetilde{\mathbb{B}}_K$. Most of the analysis developed for each of these three methods however extends to the general HMM method.

### 4.1. *Coercivity and convergence of HMM methods*

HMM methods are built on inner products and are therefore unconditionally coercive (under natural and not very restrictive assumptions on the mesh regularity). As a consequence and since they are linearly exact, they enjoy nice stability and convergence properties. The path of convergence described in Sec. 1.2 has been

[e] i.e. the matrix $\mathbb{M}_K$ such that $[F_K, G_K]_K = G_K^T\mathbb{M}_K F_K$.

successfully applied to HMM methods in Refs. 52, 74. Assuming that $\overline{u}_b = 0$ and taking $v = u$ in the discrete variational formulation (4.9) gives a natural discrete $H_0^1$ norm (the square root of the left-hand side of the equation), for which one can establish a Poincaré inequality and a discrete Rellich theorem. The convergence of HMM schemes therefore holds even if $\Lambda$ is discontinuous and $\overline{u}$ only belongs to $H^1$. For simplicial meshes, the stabilisation term in (4.3) can be removed[52] (i.e. $\mathbb{B}_K = 0$) without losing the coercivity, although numerical results are then slightly less accurate.

Nevertheless, numerical tests[28, 74] indicate that the choice of $\mathbb{B}_K$ usually plays little role in the accuracy of the scheme, provided that this matrix is scaled accordingly to some measure of the eigenvalues of $\Lambda_K$ (e.g. the trace of this tensor) and that its coercivity properties incorporate geometric information such as face sizes[54] in case of very distorted meshes[110]. Let us however notice that, in some cases, $\mathbb{B}_K$ can be selected to ensure the monotony of the HMM method (see Sec. 4.2).

This analysis of HMM method has been extended to convection-diffusion equations[19], with various discretisations of the convection term (centred, upwind, mimetic-based[32]). General forms of "automated upwinding" of the convection, scaled by the local diffusion strength, are studied in Ref. 19 and shown to be accurate in all regimes (diffusion- or convection-dominated). Numerical experiments also show that much better results are obtained, in case of strong anisotropy and heterogeneity in a convection-dominated regime, if the upwinding is made with edge unknowns rather than cell unknowns (see also Ref. 51 for the Navier-Stokes equations). This is probably general to many methods involving edge unknowns, but this would need to be theoretically and numerically investigated in a more thorough way.

As HMM methods are based on full gradients reconstructions $\mathbf{v}_K(F_K)$ or $\nabla_K u$, they are particularly well-suited to non-linear equations and have been adapted to a number of meaningful models such as fully non-linear equations of the Leray-Lions type[50] (appearing in particular in models of non-newtonian fluids), miscible flows in porous media[34] or the Navier-Stokes equations[53]. Since the technique in Sec. 1.2 neither relies on the linearity of the equation nor on the regularity of the solution, complete convergence analyses of HMM methods for these models are successfully carried out in these references (along with benchmarking), under assumptions compatible with applications.

A cell-centred modification (the SUCCES scheme) of the HMM method, eliminating the edge unknowns by computing them as convex combinations of cell unknowns, has been proposed and analysed in Ref. 74 for (1.1) and in Ref. 73 for non-linear elliptic equations. This modification ends up with less unknowns than the HMM method (only cell unknowns) and is still unconditionally coercive, but it has a larger stencil than MPFA methods and it displays less accurate numerical results on grids provoking numerical locking or if $\Lambda$ is discontinuous[72] (in this latter case, accuracy issues can be mitigated by retaining edge unknowns at the discontinuities, giving rise to the SUSHI scheme).

When $(\boldsymbol{x}_K)_{K\in\mathcal{M}}$ are the centres of gravity of the cells, HMM methods are the

original (edge-based) MFD methods and all results on these methods apply to HMM methods, for example: convergence rates for smooth data and super-convergence of $u$ if a proper lifting of the numerical fluxes exists[25, 27], *a posteriori* estimators usable for mesh refinement[18, 21], higher order methods designed to recover optimal orders of convergence on the fluxes[20, 22, 85], or extension to non-planar faces[26, 27, 114]. We will not delve into more details here and we refer to Ref. 111 for a comprehensive review of MFD methods. One open issue however seems interesting to mention regarding the extensions of MFD methods which introduce additional flux unknowns (higher order methods or methods for non-planar faces). These methods are based on the construction of local scalar products satisfying a generalisation of the consistency relation (4.6) on the expanded flux space. Algebraic decomposition of these scalar product matrices are known[22, 27], but the question remains open to find expression of these products purely based on geometrical quantities such as in (4.3). This would in particular eliminate the need to solve local algebraic problems to construct them.

**Remark 4.3 (Mixing MPFA and HMM ideas).** In Refs. 11, 76, the sub-cells flux continuity of the MPFA methods is combined with the gradient and stabilisation (4.7)-(4.8) of HMM methods (on the same sub-cells, by introducing half-edge unknowns) to construct an unconditionally coercive and convergent scheme. If the mesh and diffusion tensors are not too skewed, the sub-cells can be defined using particular harmonic edge points (instead of $\overline{\boldsymbol{x}}_\sigma$), where the solution can be interpolated using only the two neighbouring cell values. In this case, the half-edge unknowns can be eliminated vertex by vertex, as in the O-method, and a 9-point stencil cell-centred scheme is recovered on quadrilateral meshes.

Another mixing of MPFA and HMM ideas can be found in the method presented in Ref. 116. This method uses, as the MPFA O-method, additional face unknowns (as many on $\sigma$ as the number of vertices of $\sigma$) but constructs local "scalar products" in each sub-cell around a given vertex, trying to satisfy the local consistency conditions (4.6). Except on simplicial meshes, construction of such consistent coercive scalar products is not theoretically proved, but when they exists their block structure around each vertex allows one, as in the O-method, to eliminate the face unknowns and obtain a coercive method with the same stencil as the O-method.

**Remark 4.4 (Mixing HMM, MPFA and dG ideas).** Ref. 46 proposes a scheme which mixes HMM, MPFA and dG ideas. This method consists in constructing a finite-dimensional subspace $V_h$ of piecewise affine functions, whose gradient in each cell is given by (4.7) in which the edge unknowns are computed from cell unknowns using the elimination technique of the MPFA L-method. This space $V_h$ is then used in a Finite-Element like discretisation of (1.5) with a bilinear form including jumps penalisations as in dG methods.

If the edges unknowns are not eliminated then numerical fluxes can be found[47] such that this scheme satisfies the balance and conservativity equations (1.9)-(1.10).

### 4.2. *Maximum principle for HMM methods*

HMM methods are usually not monotone, even on parallelogram meshes and for constant $\Lambda$. In simple cases, one can obtain necessary and/or sufficient conditions on the diffusion tensor and the mesh for the existence (i.e. a choice of $\mathbb{B}_K$) of a monotone HMM method[112, 113]. The idea is to hybridise the method (i.e. eliminate the cell unknowns, see Sec. 4.4) and to analyse if the corresponding matrix is an M-matrix and if the corresponding right-hand side is non-negative whenever $f \geq 0$.

For simplicial meshes, a necessary and sufficient condition of monotony of any HMM method is that $\Lambda_K \mathbf{n}_{K,\sigma} \cdot \mathbf{n}_{K,\sigma'} < 0$ for all $K \in \mathcal{M}$ and all $\sigma \neq \sigma' \in \mathcal{E}_K$ (if $\Lambda$ is isotropic, this comes down to imposing that all angles of the simplicial meshes are less that $\pi/2$). *Necessary* monotony conditions can be written for meshes made of parallelograms or parallelepipeds, which turn out to be identical to the conditions in 2D for 9-point cell-centred schemes[123]. These conditions give insights on how to construct, using the algebraic point of view of MFD methods, the matrices of the local scalar products $[\cdot,\cdot]_K$ in (4.3), but remain to be translated into *geometric* constructions of proper $\mathbb{B}_K$ matrices. Although similar conditions can also be written for other types of meshes, such as locally refined rectangular meshes[112], a more thorough analysis remains to be done to find necessary and/or sufficient monotony conditions for HMM methods on generic meshes. Ref. 113 suggests, in the absence of such an analysis, to use a heuristic based on constructing $\mathbb{B}_K$ by solving local optimisation problems which penalise the scalar products $[\cdot,\cdot]_K$ whose matrix is not an M-matrix.

### 4.3. *Coercivity vs. Monotony vs. Accuracy*

If a scheme's matrix has negative eigenvalues, any negative mode will be amplified when the scheme is applied to a transient equation, thus provoking the explosion of the solution. Fig. 3 illustrates this phenomenon when a (non-coercive) G-scheme and a time-implicit discretisation (involving 150 time steps) is applied with $\Omega = (0,1)^2$ and final time $T = 0.1$ to $\partial_t \overline{u} - \mathrm{div}(\Lambda \nabla \overline{u}) = 0$ with $\overline{u}_b = 0$ and

$$\Lambda(x,y) = \frac{1}{x^2+y^2}\begin{pmatrix} 10^{-3}x^2 + y^2 & (10^{-3}-1)xy \\ (10^{-3}-1)xy & x^2 + 10^{-3}y^2 \end{pmatrix}, \quad u(0,\cdot) = \begin{cases} 1 & \text{on } (\frac{1}{4},\frac{3}{4})^2, \\ 0 & \text{elsewhere.} \end{cases}$$

The coercivity of a scheme does not only ensure that it converges as the mesh is refined, but also that it does not explode in transient cases as shown for the HMM method in Fig. 3 (the HMM solution is quite close to the expected solution in this test case).

The convergence insured by the coercivity of a method however does not mean that it is always accurate (only that it is accurate as the mesh size tends to 0). For instance, the unconditionally coercive HMM method may display very bad numerical behaviour in presence of strong misalignment between the grid directions and the principal directions of diffusion. In Fig. 4, we present the numerical solutions produced by an HMM method and the G-scheme for the constant diagonal tensor

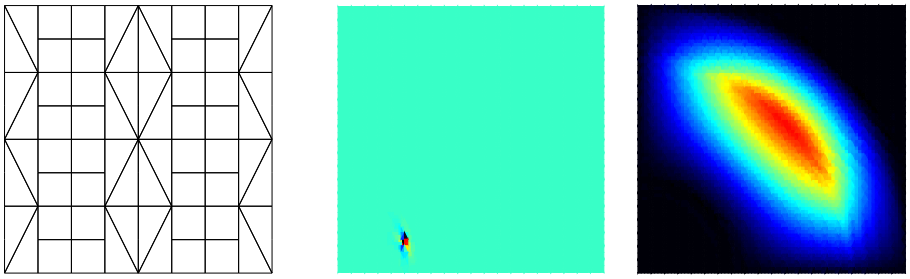

Mesh pattern (mesh=$10 \times 10$ reproduction of this pattern) | G-scheme solution, $\min u = -9 \times 10^{240}$, $\max u = 7 \times 10^{240}$ | HMM solution, $\min u = -7.9 \times 10^{-3}$, $\max u = 0.52$

Fig. 3. Explosion of a non-coercive method applied to a transient problem.

$\Lambda = \mathrm{diag}(10^4, 1)$ and the exact solution $\overline{u}(x, y) = x(1-x)y(1-y)$. The strong oscillations displayed by the HMM method in this example are probably due to its lack of monotony properties and to its non-local computations of the numerical fluxes ($F_{K,\sigma}$ is expressed in term of *all* the edge unknowns around $K$, not just unknowns around $\sigma$). Although it can be checked that the G-scheme is *not* coercive (and therefore not monotone) on this test case, its local computation of the fluxes prevents its solution from presenting spurious oscillations, and therefore seems to improve its "apparent" monotony properties.

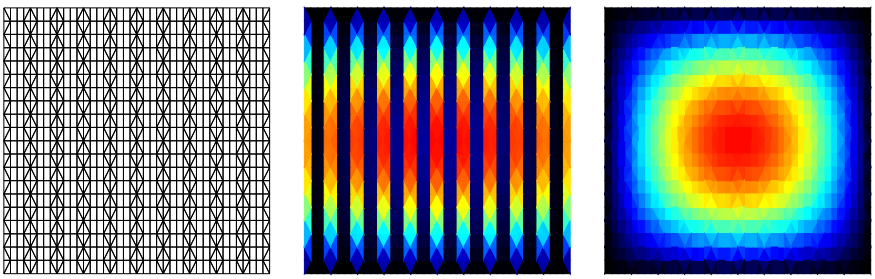

Mesh | HMM | G-scheme

Fig. 4. Numerical test with strong anisotropy ratio. The G-scheme is not coercive in this test case.

### 4.4. *To summarise: HMM methods*

The strength of HMM methods is their unconditional coercivity, on any mesh and for any diffusion tensor. This is achieved at the cost of a larger number of unknowns (cell and edge unknowns) than in MPFA methods, but hybridisation techniques can be applied as in Mixed Finite Element methods to locally eliminate the cell

unknowns and retain only the edge unknowns. This unconditional coercivity ensures the robustness of HMM methods (no explosion for transient equations) and provides the means for full convergence analyses for a vast range of different complex models, involving non-linearities and non-smooth data and solutions.

HMM methods are however not always monotone and, despite the large freedom in their construction (through the choice of the matrices $\mathbb{B}_K$), the analysis of their monotony range is to date very limited. Another weakness is their relative non-local computation of the fluxes, as $F_{K,\sigma}$ depends on all edge unknowns around $K$. Because of this, they may present inaccurate results on coarse meshes in presence of strong anistropy – although their unconditional coercivity ensures that, as the mesh is refined, the approximate solution converges to the exact solution.

The question still remains to find a FV method which would be unconditionally coercive and monotone on any type of mesh...

## 5. DDFV methods

Discrete Duality Finite Volume (DDFV) methods have been introduced around the early 2000's[88−90], but have been mostly studied after 2005[17, 24, 48]. The basic idea of DDFV methods in 2D is a bit similar to MPFA methods and also draws some inspiration from Ref. 42. The initial remark is that the two values $u_K$ and $u_L$ around $\sigma$ only give an approximation of the local gradient in the direction $(\boldsymbol{x}_K\boldsymbol{x}_L)$ and are therefore insufficient to obtain an expression of the whole gradient around $\sigma$ (when the orthogonality condition (2.5) does not hold, the whole gradient is required to compute an approximate flux $F_{K,\sigma}$). So, as in MPFA methods, DDFV methods introduce new unknowns to get an approximation of the gradient in another direction than $(\boldsymbol{x}_K\boldsymbol{x}_L)$. Using these approximate projections of the gradient on two independent directions, an approximation of the whole gradient can be reconstructed in a similar way as (3.1) defines the gradient (3.2) in MPFA methods.

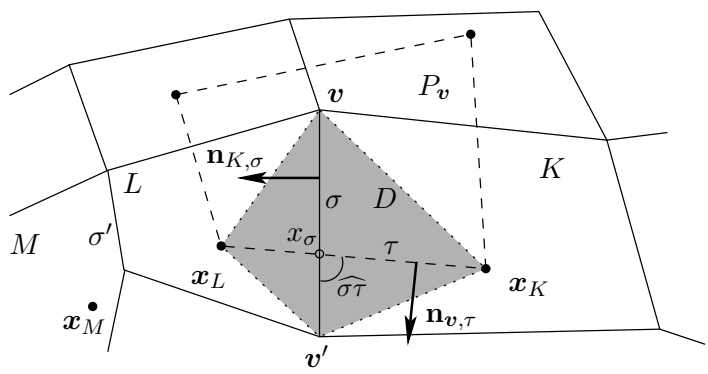


Fig. 5. DDFV primal meshes (continuous lines: $K$, $L$, $M$), dual meshes (dashed lines: $P_{\boldsymbol{v}}$) and diamonds (filled: $D$). $\mathbf{n}_{K,\sigma}$ and $\mathbf{n}_{\boldsymbol{v},\tau}$ = unit normals to $\sigma = [\boldsymbol{v}, \boldsymbol{v}']$ and $\tau = [\boldsymbol{x}_K, \boldsymbol{x}_L]$.

The additional unknowns of DDFV methods are located at the vertices of the mesh (we denote by $\mathcal{V}$ the set of vertices and we refer to Fig. 5 for notations). From the cell $(u_K)_{K\in\mathcal{M}}$ and vertex $(u_{\boldsymbol{v}})_{\boldsymbol{v}\in\mathcal{V}}$ unknowns and since $\overrightarrow{\boldsymbol{v}\boldsymbol{v}'}$ and $\overrightarrow{\boldsymbol{x}_K\boldsymbol{x}_L}$ are linearly independent, a constant approximate gradient $\nabla_D u$ can be computed on the diamond $D := \mathrm{co}(\sigma\cup\{\boldsymbol{x}_K\})\cup\mathrm{co}(\sigma\cup\{\boldsymbol{x}_L\})$([f]) by imposing $\nabla_D u\cdot(\boldsymbol{x}_K-\boldsymbol{x}_L) = u_K-u_L$ and $\nabla_D u\cdot(\boldsymbol{v}-\boldsymbol{v}') = u_{\boldsymbol{v}} - u_{\boldsymbol{v}'}$, which leads to[17, 48]

$$\begin{aligned}\nabla_D u &= \frac{1}{\sin(\widehat{\sigma\tau})}\left(\frac{u_L-u_K}{\mathrm{d}(\boldsymbol{x}_K,\boldsymbol{x}_L)}\mathbf{n}_{K,\sigma} + \frac{u_{\boldsymbol{v}'}-u_{\boldsymbol{v}}}{\mathrm{d}(\boldsymbol{v},\boldsymbol{v}')}\mathbf{n}_{\boldsymbol{v},\tau}\right)\\ &= \frac{1}{2|D|}\left((u_L-u_K)\mathrm{d}(\boldsymbol{v},\boldsymbol{v}')\mathbf{n}_{K,\sigma} + (u_{\boldsymbol{v}'}-u_{\boldsymbol{v}})\mathrm{d}(\boldsymbol{x}_K,\boldsymbol{x}_L)\mathbf{n}_{\boldsymbol{v},\tau}\right),\end{aligned} \tag{5.1}$$

where $\widehat{\sigma\tau}$ is the angle between the straight lines $(\boldsymbol{x}_K\boldsymbol{x}_L)$ and $(\boldsymbol{v}\boldsymbol{v}')$ and $|D|$ is the area of $D$. One can then compute an approximate flux through $\sigma$:

$$F_{K,\sigma} = -|\sigma|\Lambda_D\nabla_D u\cdot\mathbf{n}_{K,\sigma}, \tag{5.2}$$

where $\Lambda_D$ is the mean value of $\Lambda$ on $D$. The balance equations on each cell (1.9) then give as many equations as the number of cell unknowns. To close the system, it remains to find as many equations as the number of vertex unknowns, which is simply done by writing the balance equation on new cells ("dual cells") constructed around vertices. A natural choice[17, 24, 48, 89] for the dual cell around $\boldsymbol{v}$ is the polygon $P_{\boldsymbol{v}}$ which has all the cell points $\boldsymbol{x}_K, \boldsymbol{x}_L, \ldots$ around $\boldsymbol{v}$ as vertices (in dotted lines in Fig. 5). The flux through the edge $\tau = [\boldsymbol{x}_K, \boldsymbol{x}_L]$ of $P_{\boldsymbol{v}}$ can be computed using the gradient on $D$:

$$F_{\boldsymbol{v},\tau} = -|\tau|\Lambda_D\nabla_D u\cdot\mathbf{n}_{\boldsymbol{v},\tau} \tag{5.3}$$

and the balance of these fluxes around a vertex $\boldsymbol{v}$ reads

$$\sum_{\tau\in\mathcal{E}_{P_{\boldsymbol{v}}}} F_{\boldsymbol{v},\tau} = \int_{P_{\boldsymbol{v}}} f(x)\mathrm{d}x. \tag{5.4}$$

where $\mathcal{E}_{P_{\boldsymbol{v}}}$ is the set of all edges of $P_{\boldsymbol{v}}$. These balance equations around each vertex complete the set of equations which define the DDFV method, that is (1.9)-(5.1)-(5.2)-(5.3)-(5.4). Note that the flux conservativity across primal $\sigma$ and dual $\tau$ edges are naturally satisfied by (5.2) and (5.3).

**Remark 5.1.** Dirichlet or Neumann boundary conditions are handled seamlessly. The diamond around a boundary edge $\sigma\in\mathcal{E}_K\cap\mathcal{E}_{\mathrm{ext}}$ is only made of the triangle $\mathrm{co}(\sigma\cup\{\boldsymbol{x}_K\})$, and the gradient on $D$ is constructed by replacing $\boldsymbol{x}_L$ with a point $\boldsymbol{x}_\sigma\in\sigma$ (which is also used to define the dual cell around $\boldsymbol{v}$) and $u_L$ with some unknown $u_\sigma$. Dirichlet boundary conditions then fix $(u_\sigma)_{\sigma\in\mathcal{E}_{\mathrm{ext}}}$ and $(u_{\boldsymbol{v}})_{\boldsymbol{v}\in\mathcal{V}\cap\partial\Omega}$ using the values of $\overline{u}_b$, and (5.4) is not written for boundary vertices[17, 48]. Neumann

[f] "co" denotes the convex hull. Note that the diamond $D$ may be non-convex (this is the case for the diamond around $\sigma'$ in Fig. 5).

boundary conditions simply impose the value of $F_{K,\sigma}$, and (5.4) is written for all vertices[48].

The preceding construction is valid if all dual cells $(P_{\boldsymbol{v}})_{\boldsymbol{v}\in\mathcal{V}}$ have disjoint interiors and, therefore, form a partition $\Omega$. It may happen for peculiar meshes that the preceding construction of $P_{\boldsymbol{v}}$ leads to overlapping dual cells. In this case, the scheme must be modified and a possible choice[90] is to take for $P_{\boldsymbol{v}}$ the interaction region around $\boldsymbol{v}$ from the MPFA methods (see Fig. 2).

If $\Lambda$ is discontinuous across $\sigma$, the usage of its mean value on $D$ in (5.2) and (5.3) may lead to a loss of accuracy. In case this case, and still assuming that $\Lambda$ is constant on each (primal) cell $K \in \mathcal{M}$, the DDFV scheme can be modified[90] by introducing an unknown $u_\sigma$ at the point $\{\boldsymbol{x}_\sigma\} = \sigma \cap (\boldsymbol{x}_K\boldsymbol{x}_L)$ (or $\overline{\boldsymbol{x}}_\sigma$ if $D$ is not convex and $P_{\boldsymbol{v}}$ is the same interaction region as in MPFA methods), using it to compute constant gradients in each half-diamond $D \cap K$ and $D \cap L$ and then eliminating it thanks to the flux conservativity (1.10) through primal edges. Since there is no jump of $\Lambda$ through $\tau = [\boldsymbol{x}_K, \boldsymbol{x}_L]$, the conservativity through this dual edge is ensured as the sub-fluxes through $[\boldsymbol{x}_K, \boldsymbol{x}_\sigma]$ and $[\boldsymbol{x}_\sigma, \boldsymbol{x}_L]$ use the same values of $\Lambda$ on each side of $\tau$ (respectively $\Lambda_K$ and $\Lambda_L$) and the same gradient on each half diamond. If $\Lambda$ is also discontinuous across dual edges (which is not standard in reservoir engineering), a further modification of the DDFV method has been proposed in Ref. 24. This "m-DDFV" method uses local gradients which are constant in quarters of diamonds. Four new unknowns need to be introduced in each diamond, and are then eliminated by imposing (as in MPFA methods) flux conservativity equations through the diamond diagonals.

Although this presentation of DDFV methods clearly shows that they are based on FV principle (flux conservativity and balance), it does not explain the name "Discrete Duality Finite Volume". DDFV methods can be re-cast using discrete gradient and divergence operators, in such a way that the Green-Stokes duality formula holds at the discrete level[17, 24, 48]. The gradient operator, already defined, takes cell and vertex values (assumed to represent piecewise constant functions in primal and dual cells) and constructs a piecewise constant gradient on the diamonds. The divergence operator takes a piecewise constant vector field $(\xi_D)_D$ on diamonds and defines its divergence as piecewise constant functions on primal and dual cells by writing the flux balances (1.9) and (5.4) with $F_{K,\sigma} = |\sigma|\xi_D \cdot \mathbf{n}_{K,\sigma}$ and $F_{\boldsymbol{v},\tau} = |\tau|\xi_D \cdot \mathbf{n}_{\boldsymbol{v},\tau}$. Under this form, DDFV methods are based on similar principles as MFD methods, which aim at satisfying the discrete Green-Stokes formula (4.6). They are different methods but DDFV methods can be re-cast in a framework similar to MFD methods[40].

Generalisation of DDFV methods to 3D is based on similar ideas as in the 2D case, but requires quite heavy notations to be properly defined. Two essentially different 3D generalisations exist: methods using Cell and Vertex unknowns (hence dubbed CeVe-DDFV) and methods relying on Cell, Vertex, Faces and Edges unknowns (called CeVeFE-DDFV). Refs. 92, 41, 15 design CeVe-DDFV methods by

reconstructing a piecewise constant gradient from its projection on $\overrightarrow{\boldsymbol{x}_K\boldsymbol{x}_L}$ computed using $u_K$ and $u_L$, and its projection on the plane generated by $\sigma$ computed using the values on the vertices of $\sigma$. Linearly exact formulas can be found for this projected gradient[14] but the discrete Poincaré inequality (crucial to Step (C1) in Sec. 1.2) only seems provable when all faces $\sigma$ are triangles([g]) and the CeVe-DDFV method is therefore not coercive on generic meshes. Refs. 38, 39 propose a CeVeFE-DDFV method with a local gradient computed from its projection on $\overrightarrow{\boldsymbol{x}_K\boldsymbol{x}_L}$ and $\overrightarrow{\boldsymbol{v}\boldsymbol{v}'}$ (as in 2D) and on a third face-edge direction. A third mesh is built around each face and edge centres to obtain additional balance equations for the new face and edge unknowns. This CeVeFE-DDFV method is coercive on any mesh, but at the cost of additional unknowns with respect to the CeVe-DDFV method.

### 5.1. *Coercivity and convergence of DDFV methods*

Because DDFV methods are based on discrete gradient and divergence operators which reproduce, as MFD methods, the Green-Stokes formula, discrete $H_0^1$ estimates can be obtained by mimicking the continuous integration by parts (1.11), provided that the discrete Poincaré inequality holds. This is the case in 2D, for the CeVeFE-DDFV 3D method or for the CeVe-DDFV 3D method on meshes with triangular faces. In these cases, DDFV methods are coercive and, being linearly exact, they enjoy the corresponding stability and convergence properties.

The technique outlined in Sec. 1.2 has been applied[17] to prove the convergence, without additional regularity assumption on the data or the solution, of the 2D DDFV method using the mean values $\Lambda_D$ as in (5.2)-(5.3) (Ref. 17 provides in fact a convergence analysis for a non-linear equation, which contains (1.1) as a particular case). An $\mathcal{O}(h_{\mathcal{M}})$ error estimate for $u$ and the discrete gradient are also established if $\Lambda$ is Lipschitz-continuous and $\overline{u} \in H^2$ (this estimate was known[48] for $\Lambda = \mathrm{Id}$).

Concerning the m-DDFV method[24, 90], an $\mathcal{O}(h_{\mathcal{M}})$ error estimate for $\overline{u}$ and its gradient has been proved in Ref. 24 (also for a non-linear version of (1.1)), provided that $\overline{u}$ is $H^2$ on each half- or quarter-diamond. This regularity assumption does not seem always satisfied (in particular if $\Omega$ or some cells around discontinuities of $\Lambda$ are not convex), but the path described in Sec. 1.2 could also be applied to the m-DDFV method.

An $\mathcal{O}(h_{\mathcal{M}})$ error estimate on $\overline{u}$ has been obtained in Ref. 38 for the 3D CeVeFE-DDFV method, under the assumptions that $\Lambda$ is Lipschitz-continuous and that $\overline{u} \in H^2(\Omega)$. We can however notice that this CeVeFE-DDFV method (as well as the 2D DDFV scheme) is a Gradient Scheme[76] and, therefore, that its convergence without regularity assumptions, for (1.1) as well as non-linear and non-local equations, follows from the general convergence analysis of Gradient Schemes[55, 76].

As HMM methods, DDFV methods have been adapted to more complex models than (1.1): non-linear elliptic equations[17, 24, 38], stationary and transient convection-

[g]Or on cartesian grids[13].

diffusion equations[40, 93], the cardiac bidomain model[16], div-curl problems[44, 91], degenerate hyperbolic-parabolic problems[15] (with assumptions on the mesh, see Sec. 5.2), the linear Stokes equations with varying viscosity[100, 101], semiconductor models[33] and the Peaceman model[36]. The convergence analysis of DDFV methods is carried out (sometimes under regularity assumptions) for all these models except the last two. Analysis tools for the 3D CeVe-DDFV method are presented in Ref. 13, 14 and used to study its convergence for transient non-linear equations or systems.

### 5.2. *Maximum principle for DDFV methods*

On meshes satisfying the orthogonality conditions (2.1) or (2.5), DDFV methods for (1.1) are identical to two TPFA schemes[48] (one on each primal and dual mesh), and are therefore monotone. This monotony under orthogonality conditions on the mesh is used in Ref. 15 to study DDFV discretisations of degenerate hyperbolic-parabolic equations, and in particular to establish discrete entropy inequalities on approximate solutions. Study of the monotony of DDFV methods on generic meshes however remains to be done.

### 5.3. *To summarise: DDFV methods*

As HMM methods, the main strength of DDFV methods is their unconditional coercivity (with some caveats for 3D methods, see above), which ensures their robustness and allows one to adapt them and analyse their convergence for a number of models. Another very practical property for the analysis of DDFV methods is their discrete duality property (existence of discrete gradient and divergence operators satisfying Stokes' formula), which is also shared by HMM methods. An advantage of DDFV methods over HMM methods is perhaps their more local computation of the fluxes ($F_{K,\sigma}$ is expressed in terms of unknowns localised around the edge $\sigma$, whereas in HMM methods this flux requires all edge unknowns around $K$).

A relative weakness of DDFV methods is their intricacy in 3D. The heavy and numerous notations required for the definitions of 3D DDFV methods probably makes them difficult to adopt by non-specialists and complexifies their analysis. In particular, establishing the discrete duality formula is far from obvious. Once passed these complicated notations, however, implementation of 3D DDFV methods is not particularly difficult. The lack of monotony studies for DDFV methods is also a gap in the literature, which would probably need to be filled to get a better understanding on the possible applicability of these methods to multi-phase flow models.

And so our quest for an unconditionally coercive and monotone FV method on any mesh continues...

## 6. Monotone and Minimum-Maximum preserving (MMP) methods

Previously cited results[96, 97, 122, 123] show that no *linear* 9-point scheme on quadrangular meshes, exact for linear functions (i.e. of formal order 2), can be monotone on any distorted mesh or for any diffusion tensor. Some constraints must be relaxed... One choice is to allow for larger stencils (see Ref. 106 for a Finite Difference scheme). For Finite Volume methods, the most common choice appears to be a relaxation of the *linearity* of the scheme and the construction of *non-linear* "monotone" approximations of the linear equation (1.1). The obvious trade-of is that computing the solution to the scheme will be more complex, requiring Picard or Newton iterations, which may create computational issues (such as the choice of stopping criteria). Also, the monotony, conservativity and/or consistency may only be achieved for the genuine solution to the non-linear scheme, not at each iteration of these algorithms[105].

Contrary to MPFA, HMM or DDFV methods, schemes presenting discrete minimum-maximum principles do not form a well defined family of methods but are rather schemes constructed using similar ideas and trying to achieve the discrete minimum principle (1.17) or the discrete minimum-maximum principle (1.18). As we are considering non-linear schemes, these two principles are not equivalent and we should make sure that we clearly separate both. Schemes satisfying (1.17) will be called *monotone*, as a commonly used but somewhat misguided extension of the vocabulary used for linear schemes([h]), whereas schemes which satisfy (1.18) will be called *minimum-maximum preserving* (MMP) schemes.

A widespread idea to obtain a monotone or MMP scheme is to compute two *linear* fluxes $F^1_{K,\sigma}$ and $F^2_{K,\sigma}$ for each interior edge and to define $F_{K,\sigma}$ as a convex combination of $F^1_{K,\sigma}$ and $F^2_{K,\sigma}$ with coefficients depending upon the unknown $u$:

$$\begin{aligned} &F_{K,\sigma} = \mu^1_{K,\sigma}(u)F^1_{K,\sigma} + \mu^2_{K,\sigma}(u)F^2_{K,\sigma} \\ &\text{with } \mu^1_{K,\sigma}(u) \geq 0,\ \mu^2_{K,\sigma}(u) \geq 0 \text{ and } \mu^1_{K,\sigma}(u) + \mu^2_{K,\sigma}(u) = 1. \end{aligned} \tag{6.1}$$

The methods we consider here are cell-centred, but the definition of $F^1_{K,\sigma}$ and $F^2_{K,\sigma}$ may require to introduce additional unknowns (e.g. vertex, edge or other unknowns). These unknowns are then eliminated, classically by expressing them as convex combinations of cell unknowns. The coefficients $\mu^1_{K,\sigma}(u)$ and $\mu^2_{K,\sigma}(u)$ are chosen to eliminate the "bad" parts of $F^1_{K,\sigma}$ and $F^2_{K,\sigma}$, responsible for the possible loss of monotony.

[h]Indeed, "monotone" non-linear methods do not necessarily preserve orders of boundary conditions or of initial condition for time-dependent problems. They merely provide solutions which remain non-negative when the boundary/initial conditions are non-negative.

### 6.1. *Non-linear "2pt-fluxes": monotone schemes*

The TPFA scheme is monotone thanks to its "2pt-flux" structure. This suggests to try and build monotone methods on generic meshes by computing $F_{K,\sigma}$ with a "2pt" formula, involving apparently only $u_K$ and $u_L$ but with coefficients depending on all cell unknowns and boundary values $U = ((u_M)_{M\in\mathcal{M}}, (u_\sigma)_{\sigma\in\mathcal{E}_{\rm ext}})$ (same notation as in Sec. 1.3). Indeed, assume that $F_{K,\sigma}$ is written

$$F_{K,\sigma} = \alpha_{K,L}(U)u_K - \beta_{K,L}(U)u_L \quad \text{with } \alpha_{K,L}(U) > 0 \text{ and } \beta_{K,L}(U) > 0 \tag{6.2}$$

(where $L$ is the cell on the other side of $\sigma \in \mathcal{E}_K \cap \mathcal{E}_{\rm int}$ and $L = \sigma$ whenever $\sigma \in \mathcal{E}_K \cap \mathcal{E}_{\rm ext}$). Then the conservativity relation (1.10) imposes, assuming that it must be satisfied for any value of $U$,

$$\alpha_{K,L}(U) = \beta_{L,K}(U) \text{ for any neighbour cells } K \text{ and } L. \tag{6.3}$$

The scheme (1.9) can then be recast as

$$A(U)(u_K)_{K\in\mathcal{M}} = (B_K(U))_{K\in\mathcal{M}}, \tag{6.4}$$

where $B_K(U) = \int_K f(x)\mathrm{d}x + \sum_{\sigma\in\mathcal{E}_{\rm ext}\cap\mathcal{E}_K} \beta_{K,\sigma}(U)u_\sigma$ and the matrix $A(U)$ has (i) diagonal coefficients $A_{K,K}(U) = \sum_M \alpha_{K,M}(U) > 0$ (the sum being on all $M$ neighbour cells or edges of $K$), (ii) extra-diagonal coefficients $A_{K,L}(U) = -\beta_{K,L}(U) < 0$ if $K$, $L$ are neighbour cells, $A_{K,L}(U) = 0$ otherwise, and (iii) is diagonally dominant by column (strictly for columns $L$ such that $\mathcal{E}_{\rm ext} \cap \mathcal{E}_L \neq \emptyset$) thanks to (6.3). The graph of $A(U)$ is also connected and (cf. Sec. 1.3) $A(U)^{-1}$ therefore has non-negative coefficients, which means that the scheme (6.4) satisfies (1.17).

#### 6.1.1. *Triangular meshes*

A first idea[103] to achieve (6.2) via (6.1) on 2D triangular meshes is to compute, for each interior edge $\sigma$ and each $i = 1, 2$, a constant gradient $\nabla_i u$ on the triangle $T_i = \boldsymbol{v}_i\boldsymbol{x}_K\boldsymbol{x}_L$ (see notations in Fig. 6) by using unknown values $(u_{\boldsymbol{v}_i}, u_K, u_L)$ at this triangle vertices. These gradients are given by (3.2) with $\boldsymbol{x}_K$ replaced by $\boldsymbol{v}_i$ and $\overline{\boldsymbol{x}}_\sigma, \overline{\boldsymbol{x}}_{\sigma'}$ replaced by $\boldsymbol{x}_K, \boldsymbol{x}_L$ and, assuming $\Lambda = \mathrm{Id}$, the linear conservative fluxes $F^i_{K,\sigma}$ $(i = 1, 2)$ are then[103, 115]

$$F^i_{K,\sigma} := -|\sigma|\nabla_i u \cdot \mathbf{n}_{K,\sigma} = \frac{|\sigma|}{2|T_i|}\left(u_K\nu^L_i + u_L\nu^K_i - u_{\boldsymbol{v}_i}(\nu^K_i + \nu^L_i)\right) \cdot \mathbf{n}_{K,\sigma} \tag{6.5}$$

where $|T_i|$ is the area of triangle $T_i$. The convex combination (6.1) is then designed to eliminate, in $F_{K,\sigma}$, the term

$$-\frac{|\sigma|}{2}\left(\frac{\mu^1_\sigma(u)(\nu^K_1 + \nu^L_1)\cdot\mathbf{n}_{K,\sigma}}{|T_1|}u_{\boldsymbol{v}_1} + \frac{\mu^2_\sigma(u)(\nu^K_2 + \nu^L_2)\cdot\mathbf{n}_{K,\sigma}}{|T_2|}u_{\boldsymbol{v}_2}\right)$$

involving $u_{\boldsymbol{v}_1}, u_{\boldsymbol{v}_2}$ and which prevents this flux from having the "2-pt structure" (6.2). As $\nu^K_1 + \nu^L_1 + \nu^K_2 + \nu^L_2 = 0$, valid choices of the coefficients are

$$\mu^1_\sigma(u) = \frac{u_{\boldsymbol{v}_2}/|T_2|}{u_{\boldsymbol{v}_1}/|T_1| + u_{\boldsymbol{v}_2}/|T_2|} \text{ and } \mu^2_\sigma(u) = \frac{u_{\boldsymbol{v}_1}/|T_1|}{u_{\boldsymbol{v}_1}/|T_1| + u_{\boldsymbol{v}_2}/|T_2|}, \tag{6.6}$$

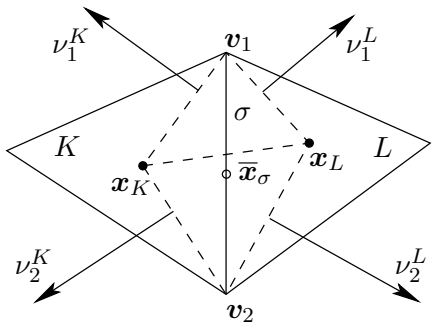


Fig. 6. Construction of a monotone scheme on triangular meshes. The vectors $\nu_i^{K/L}$ have the length of the segment to which they are orthogonal.

provided that $u_{\boldsymbol{v}_1}$ and $u_{\boldsymbol{v}_2}$ are both non-negative and not simultaneously equal to 0 (in this last case, we can still take $\mu_\sigma^1 = \mu_\sigma^2 = \frac{1}{2}$). Computing these vertex values by convex combinations of the cell unknowns ensures that they are non-negative whenever all cell unknowns are non-negative. Two combinations are suggested in Ref. 115, but none of them takes into account the possible non-smoothness of $\overline{u}$ around discontinuities of $\Lambda$ and the resulting schemes therefore suffer from a loss of consistency around these discontinuities (see Remark 6.3).

With the choices (6.5)-(6.6), it can be proved that, *provided that* $(\boldsymbol{x}_K)_{K\in\mathcal{M}}$ *are at the intersections of the bisectors of the triangles* $K \in \mathcal{M}$ (this is where the restriction on the mesh, i.e. that it is made of triangles, comes into play), $F_{K,\sigma}$ given by (6.1) indeed has the "2pt structure" (6.2) with positive coefficients.

**Remark 6.1.** This construction of fluxes only makes sense if all $u_K$ are non-negative, and the scheme's matrix $A(U)$ in (6.4) is therefore well defined only for non-negative cell unknowns. This is not a practical issue as the non-linear system (6.4) is often solved by iterating an algorithm of the form $A(U^n)(u_K^{n+1})_{K\in\mathcal{M}} = (B_K(U^n))_{K\in\mathcal{M}}$ with all components of $B_K(U^n)$ non-negative if all components of $U^n$ are non-negative. By the properties of $A(U)$, all $u_K^n$ found in these iterations are non-negative and $A(U^n)$ is therefore well defined.

The modification of this method[115] for heterogeneous anisotropic tensors $\Lambda$ consists in taking $\boldsymbol{x}_K$ at the intersection of the bisectors for the $\Lambda_K$-metric of triangle $K$ and in introducing an additional unknown $u_\sigma$ at the edge midpoint $\overline{\boldsymbol{x}}_\sigma$. Four fluxes $F_{K,\sigma}^{i,M}$ are then computed using gradients in the triangles $\boldsymbol{v}_i\boldsymbol{x}_M\overline{\boldsymbol{x}}_\sigma$ ($i = 1, 2$, $M = K, L$) and the flux continuities $F_{K,\sigma}^{i,K} = F_{K,\sigma}^{i,L}$ are written to eliminate the unknown $u_\sigma$ and to obtain two fluxes $F_{K,\sigma}^i$, which are then used in (6.1). New coefficients $\mu_\sigma^i(u)$ are found which eliminate the $u_{\boldsymbol{v}_i}$ terms and, thanks to the initial choice of $\boldsymbol{x}_K$, $F_{K,\sigma}$ has the structure (6.2).

This method has been extended to 3D tetrahedral meshes in Ref. 95 (using convex combinations of three linear fluxes instead of two) and to general 2D polygonal

meshes in Ref. 115, albeit in this last case at the expense of a loss of consistency of the method, especially for strong anisotropic tensors.

These non-linear 2pt-fluxes methods are not coercive in general and no convergence proof is provided in the literature. However, numerical tests show for smooth data a generic order of convergence 2 for the solution and 1 for its gradient. Some numerical simulations[115] also confirm that the solution does not satisfy the full discrete minimum-maximum principle (1.18) in general: the approximate solution for $f = 0$ may present values beyond the maximum of the boundary values, and even internal oscillations.

### 6.1.2. *Polygonal meshes*

Ref. 134 presents the construction of consistent 2pt-fluxes (6.2) on polygonal meshes using similar ideas to Ref. 103, 115. The starting point is, for $\sigma \in \mathcal{E}_K$, to select two vertices $\boldsymbol{v}_1, \boldsymbol{v}_2$ of $K$ such that $\Lambda_K \mathbf{n}_{K,\sigma}$ is in the positive cone generated by $\overrightarrow{\boldsymbol{x}_K \boldsymbol{v}_1}$ and $\overrightarrow{\boldsymbol{x}_K \boldsymbol{v}_2}$ (cf Fig. 7).

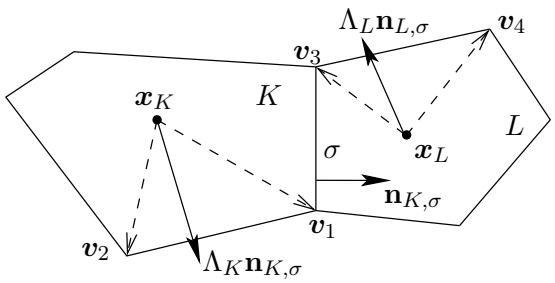


Fig. 7. Construction of a monotone scheme on polygonal meshes.

The flux through $\sigma$ outside $K$ can then be approximated by a positive combination of $-\nabla \overline{u} \cdot \overrightarrow{\boldsymbol{x}_K \boldsymbol{v}_i} \approx \mathrm{d}(\boldsymbol{x}_K, \boldsymbol{v}_i)(u_K - u_{\boldsymbol{v}_i})$ $(i = 1, 2)$ and this gives a first numerical flux $F^1_{K,\sigma} = a_{K,\sigma}(u_K - u_{\boldsymbol{v}_1}) + b_{K,\sigma}(u_K - u_{\boldsymbol{v}_2})$, with non-negative coefficients $a_{K,\sigma}$ and $b_{K,\sigma}$. The same construction from cell $L$ gives a numerical flux outside $K$ (i.e. inside $L$) $F^2_{K,\sigma} = -a_{L,\sigma}(u_L - u_{\boldsymbol{v}_3}) - b_{L,\sigma}(u_L - u_{\boldsymbol{v}_4})$ with $\boldsymbol{v}_3, \boldsymbol{v}_4$ vertices of $L$ and $a_{L,\sigma}, b_{L,\sigma}$ non-negative. The total flux is then obtained as in Refs. 103, 115 by a convex combination (6.1) designed to eliminate the coefficients of $u_{\boldsymbol{v}_i}$ and to provide the conservativity of the global flux:

$$\mu^1_{K,\sigma}(u) = \frac{a_{L,\sigma} u_{\boldsymbol{v}_3} + b_{L,\sigma} u_{\boldsymbol{v}_4}}{a_{K,\sigma} u_{\boldsymbol{v}_1} + b_{K,\sigma} u_{\boldsymbol{v}_2} + a_{L,\sigma} u_{\boldsymbol{v}_3} + b_{L,\sigma} u_{\boldsymbol{v}_4}},$$

$$\mu^2_{K,\sigma}(u) = \frac{a_{K,\sigma} u_{\boldsymbol{v}_1} + b_{K,\sigma} u_{\boldsymbol{v}_2}}{a_{K,\sigma} u_{\boldsymbol{v}_1} + b_{K,\sigma} u_{\boldsymbol{v}_2} + a_{L,\sigma} u_{\boldsymbol{v}_3} + b_{L,\sigma} u_{\boldsymbol{v}_4}}.$$

The resulting flux (6.1) is well defined provided that all $u_{\boldsymbol{v}_i}$ are non-negative (if they are all equal to 0, we take $\mu^i_{K,\sigma}(u) = 1/2$) and has the "2pt-structure" (6.2).

The vertex values $u_{\boldsymbol{v}_i}$ are computed using convex combinations of cell values as in Ref. 115 or, in case of discontinuity of $\Lambda$, by writing down the flux conservativity and the continuity of tangential gradients at the vertices. This last method however sometimes fails to provide non-negative vertex values $u_{\boldsymbol{v}_i}$ from non-negative cell values, in which case a simple convex combination must be used.

As for the methods constructed in Refs. 103, 115, no proof of convergence is provided in Ref. 134 but numerical experiments shows convergence, with rates 2 for $\overline{u}$ and 1 for the fluxes for smooth data. However, for strongly anisotropic $\Lambda$, the rate of convergence for $\overline{u}$ seems reduced, at least at available mesh sizes.

This method has been applied to advection-diffusion equations[131] (for a constant $\Lambda$), using the same kind of discretisation of the advection term as in Ref. 118, i.e. a higher order method with slopes limiters.

A variant can be constructed[127] using edge unknowns $u_\sigma$ (instead of vertices unknowns) and eliminating them as in the MPFA O-method. This process may however produce negative $u_\sigma$'s from non-negative $u_K$'s and, when this happens, $u_\sigma$ must be computed using a simple convex combination of $u_K$'s. Although the number of iterations required to compute the solution are reduced in Ref. 127 with respect to Ref. 134, it seems much higher than for the methods in Refs. 58, 105 (see Sec. 6.2), for which the number of iterations appears to remain bounded independently on the mesh size.

The ideas of Ref. 134 have also been used in Ref. 117, 118, but by expressing $\Lambda_K \mathbf{n}_{K,\sigma}$ as a positive combination of $\overrightarrow{\boldsymbol{x}_K \boldsymbol{x}_{L_i}}$, for some cell or edges $L_1, L_2$, instead of $\overrightarrow{\boldsymbol{x}_K \boldsymbol{v}_i}$ for some vertices $\boldsymbol{v}_1, \boldsymbol{v}_2$. This choice does not require to interpolate new vertex or edge unknowns, which is an advantage since such interpolations may lead to inaccuracies if not well chosen[115]. However, when $\Lambda$ is discontinuous across an edge, the cell centres on each side must be moved according to the heterogeneity of $\Lambda$ (in such a way that (2.5) holds for this edge). As a consequence, the method is applicable only if each cell has at most one edge across which $\Lambda$ is discontinuous, which restricts the number and positions of diffusion jumps. This method has been extended to general 3D polyhedral meshes in Refs. 43, 121.

### 6.2. *Non-linear multi-point fluxes: MMP schemes*

As mentioned above, methods based on the form (6.2) are monotone but do not satisfy the discrete minimum-maximum principle, mostly because they do not ensure that $\sum_L \alpha_{K,L}(U) \geq \sum_L \beta_{K,L}(U)$. It is however possible to construct, on generic 3D meshes, non-linear MMP schemes provided the fluxes are computed using a multi-point formula. More precisely, if

$$F_{K,\sigma} = \sum_{Z \in V(K)} \tau_{K,Z}(U)(u_K - u_Z) \tag{6.7}$$

with $V(K)$ a set of cells or edges and $\tau_{K,Z}(U) \geq 0$ ($> 0$ whenever $Z$ is a cell or edge around $K$), then a straightforward adaptation of the proof in Remark 2.3 shows

that the resulting scheme satisfies the discrete minimum-maximum principle (1.18) (this proof, as mentioned in Remark 2.3, demonstrates in fact that the scheme is non-oscillating). The key element is that (6.7) ensures that, whenever all cell values are equal, the fluxes are equal to 0 or have a sign opposite to the sign of $\overline{u}_b$ (this is not certain with (6.2)).

A first scheme in this direction is proposed in Ref. 23, for isotropic diffusion and under restrictive assumptions on the mesh (made of simplices), such that there exists cell points $(\boldsymbol{x}_K)_{K\in\mathcal{M}}$ satisfying the orthogonality condition (2.5). For such equations and meshes, the TPFA method can be applied but the interest of the method in Ref. 23 resides in the fact that it produces order 2 approximations *of the cell averages of* $\overline{u}$ (the TPFA method would produce order 2 approximations of $(\overline{u}(\boldsymbol{x}_K))_{K\in\mathcal{M}}$, where $(\boldsymbol{x}_K)_{K\in\mathcal{M}}$ are not at cell barycentres). Nonetheless, the particular convex combinations ideas of Ref. 23 have been used to construct MMP schemes on triangular meshes[104, 105], construction then generalised to generic 2D or 3D meshes in Ref. 58.

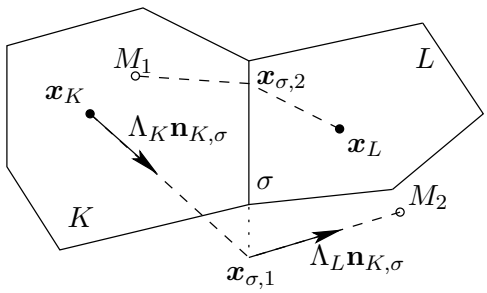


Fig. 8. Construction of an MMP scheme. $\boldsymbol{x}_{\sigma,1}$ is at the intersection of $\boldsymbol{x}_K + [0,\infty)\Lambda_K\mathbf{n}_{K,\sigma}$ and of the line/plane containing $\sigma$. $M_2$ is on the half-line $\boldsymbol{x}_{\sigma,1} + [0,\infty)\Lambda_L\mathbf{n}_{K,\sigma}$.

With the notations in Fig. 8, the scheme in Ref. 58 starts from the two consistent fluxes outside $K$:

$$\widetilde{F}^1_{K,\sigma} = |\Lambda_K\mathbf{n}_{K,\sigma}|\frac{u_K - u_{\sigma,1}}{\mathrm{d}(\boldsymbol{x}_K, \boldsymbol{x}_{\sigma,1})}\,, \quad \widetilde{F}^2_{K,\sigma} = |\Lambda_L\mathbf{n}_{K,\sigma}|\frac{u_{\sigma,1} - u_{M_2}}{\mathrm{d}(\boldsymbol{x}_{\sigma,1}, M_2)}$$

where $u_{M_2}$ and $u_{\sigma,1}$ are values at $M_2$ and $x_{\sigma,1}$ respectively. Writing the conservativity of these fluxes allows us to eliminate $u_{\sigma,1}$ and to get a linear conservative flux $F^1_{K,\sigma} = a^1_{K,\sigma}(u_K - u_{M_2})$ with $a^1_{K,\sigma} \geq 0$. Expressing $u_{M_2}$ as a convex combination of cell unknowns, in such a way that $u_L$ appears with a non-zero coefficient in this combination (this is always possible), we then get

$$F^1_{K,\sigma} = \alpha^1_{K,\sigma}(u_K - u_L) + G^1_{K,\sigma} \text{ with } G^1_{K,\sigma} = \sum_M \beta^1_{K,M}(u_K - u_M) \tag{6.8}$$

with $\alpha^1_{K,\sigma} > 0$ and $\beta_{K,M} \geq 0$. The same construction from cell $L$ gives a flux outside

$K$ (i.e. inside $L$)

$$F^2_{K,\sigma} = \alpha^2_{L,\sigma}(u_K - u_L) + G^2_{L,\sigma} \text{ with } G^2_{L,\sigma} = \sum_M \beta^2_{L,M}(u_M - u_L). \tag{6.9}$$

Following Ref. 23, a convex combination (6.1) of these two fluxes is then chosen in order to eliminate the "bad" terms with respect to (6.7), i.e. $G^2_{L,\sigma}$:

$$\mu^1_{K,\sigma}(u) = \frac{|G^2_{L,\sigma}|}{|G^1_{K,\sigma}| + |G^2_{L,\sigma}|}, \quad \mu^2_{K,\sigma}(u) = \frac{|G^1_{K,\sigma}|}{|G^1_{K,\sigma}| + |G^2_{L,\sigma}|} \tag{6.10}$$

(once again, these coefficients are chosen equal to 1/2 if their denominator vanishes). By studying separate cases depending on the sign of $G^1_{K,\sigma}G^2_{L,\sigma}$, we can then see that $F_{K,\sigma}$ defined by (6.1), (6.8), (6.9) and (6.10) always satisfies (6.7), whatever the values (positive or negative) of the cell unknowns.

**Remark 6.2.** More freedom is possible on the decompositions in (6.8) and (6.9), provided that the global non-linear flux $F_{K,\sigma}$ is continuous with respect to $u$. This is ensured[58] if we take $\alpha^1_{K,\sigma} = \alpha^2_{L,\sigma}$ (always possible, upon moving part of the term $u_K - u_L$ in (6.8) and (6.9) into $G^1_{K,\sigma}$ and $G^2_{L,\sigma}$).

This method is not necessarily coercive. However, under some coercivity assumptions (which seem satisfied in numerical tests), a rigorous proof of convergence is given in Ref. 58 without regularity assumptions on the data, drawing on the fact that the global flux is a convex combination of linear fluxes and adapting the analysis technique developed in Ref. 10. This is, to our best knowledge, the first proof of convergence of an MMP scheme. Numerical results show a general order 2 convergence for $u$ and, of course, the absence of spurious oscillations in the solution.

**Remark 6.3 (Choice of convex combination for $u_{M_i}$).** In case of jumps of $\Lambda$, numerical tests[58] show that if $u_{M_i}$ is computed from cell unknowns on both sides of a discontinuity of $\Lambda$ then the order of the scheme can be reduced (and the number of Picard iterations to compute the approximate solution increases significantly). In many applications, it is however always possible to choose $M_i$ such that $u_{M_i}$ can be computed using cell unknowns all in a same zone of smoothness of $\Lambda$.

The ideas developed for "2pt non-linear fluxes" (see Section 6.1) have also been combined with the convex combination (6.10) used in Refs. 23, 58, 103 to produce minimum-maximum preserving schemes on 2D polygonal meshes. In Ref. 126, the ideas of Ref. 134 (replacing vertex unknowns by edge unknowns) are used to built an MMP method, in which edge unknowns are interpolated from cell unknowns by writing a particular flux conservativity which takes into account the possible jumps of $\Lambda$.

Under an assumption which slightly limits the mesh's skewness and the tensor's anisotropy, Ref. 119 draws on the core idea of Ref. 117 (expressing $\Lambda_K \mathbf{n}_{K,\sigma}$ as a positive combination of $\overrightarrow{\boldsymbol{x}_K \boldsymbol{x}_{L_i}}$ for some cell or edges $L_i$) to produce an MMP scheme on 2D polygonal meshes. Using cell unknowns rather than interpolating new

vertex or edge unknowns ensures that the stencil of the linear systems solved at each Picard iteration is as small as the stencil of the TPFA method (with the trade-of that the fluxes are only conservative at the limit of these non-linear iterations). Contrary to Ref. 117, the method in Ref. 119 also does not move cell centres on each side of an edge across which $\Lambda$ is discontinuous, but rather makes use of the harmonic interpolation introduced in Ref. 11 (see Remark 4.3) to compute the flux through these edges. The usage of this harmonic interpolation however leads to a reduced accuracy if the mesh or the tensor are too skewed.

### 6.3. *MMP schemes by non-linear corrections of linear schemes*

None of the monotone or MMP method presented in the previous sections is unconditionally coercive. It turns out that the most efficient way to construct MMP *and coercive* methods is not to design a whole new method, but to take existing linear coercive methods and to devise a non-linear modification of them, which preserves its coercivity while adding the discrete minimum-maximum principle.

Let us consider a cell-centred linear scheme (1.9)-(1.10) which is coercive (it satisfies in particular (1.12)). Assume that, for this scheme,

$$A_K(u) := \sum_{\sigma\in\mathcal{E}_K} F_{K,\sigma} = \sum_{Z\in V(K)} a_{K,Z}(u_K - u_Z)$$

for some possibly negative $a_{K,Z}$ and $V(K)$ a set of cells or boundary edges such that, for two cells $(K, Z)$, $Z \in V(K)$ if and only if $K \in V(Z)$. The scheme is thus written: for all $K \in \mathcal{M}$, $A_K(u) = \int_K f(x)\mathrm{d}x$. Then a coercive MMP scheme can be obtained[31, 107] by writing $S_K(u) = \int_K f(x)\mathrm{d}x$ for all $K \in \mathcal{M}$, where

$$\begin{aligned} S_K(u) &= A_K(u) + \sum_{Z\in V(K)} \beta_{K,Z}(u)(u_K - u_Z) \\ \text{with} \quad \beta_{K,Z}(u) &\geq \frac{|A_K(u)|}{\sum_{Y\in V(K)} |u_K - u_Y|} \end{aligned}$$

("$\geq$" is replaced with "$>$" if $Z$ is a neighbouring cell or edge of $K$, and if $\sum_{Y\in V(K)} |u_K - u_Y| = 0$ then we only need $\beta_{K,Z}(u) \geq 0$; this condition on $\beta_{K,Z}$ is only an example, see Ref. 31). If $\beta_{K,Z}(u) = \beta_{Z,K}(u)$ for any cells $K, Z$, then the modified scheme is indeed a FV method: non-linear conservative fluxes $F'_{K,\sigma}(u)$ can be found such that $S_K(u) = \sum_{\sigma\in\mathcal{E}_K} F'_{K,\sigma}(u)$.

It is obvious from the symmetry of $\beta_{K,Z}(u)$ that the corrected scheme retains the coercivity property (1.12) of the original scheme. It can also be proved that, if the original scheme is consistent in the sense of FV methods, then the modified scheme converges as the mesh size tends to 0, under assumptions on the approximations not formally proved but holding well in numerical tests.

These numerical tests show astonishing improvements of the $L^2$ error when using the non-linear correction (sometimes[108] by a factor 10,000 in case of an anisotropy ratio of $10^6$). This correction however appears to degrade the order of convergence

to 1 and is therefore outperformed by the original order 2 linear scheme on very thin meshes (sometimes at a size which is nevertheless beyond computational capacities). The reason for this reduction of convergence rate is not well understood, but it is worth mentioning that, even for linear FV schemes, the convergence order 2 on $\overline{u}$ is mostly only *noticed* on numerical tests and not proved in general. The consequence is that non-linear corrections should only be applied for coarse meshes and strongly anisotropic diffusion tensors for which the original scheme provides physically unacceptable solutions.

This correction technique has been adapted in Ref. 109 to methods involving cell and edge unknowns.

## 7. Conclusion

We presented and gave a review of some recent FV methods for diffusion equations, focusing on the capacity of the methods to be applicable on generic meshes and to reproduce two important properties of the continuous equation: coercivity, which ensures the stability of the scheme and allows one to carry out convergence proofs under realistic assumptions, and minimum and maximum principles, which ensure physically acceptable solutions in case of strong anisotropy.

This review is of course partial and much more could be written on FV methods for (1.1), for example about the comparison of their respective numerical behaviours – see e.g. the two comprehensive benchmarks of Refs. 78, 87. Other methods or topics of interest regarding the discretisation of (1.1) are worth mentioning:

- vertex-centred MPFA O-methods[61, 64, 65, 124],
- Finite Volume Element methods[29, 30, 68], based on Finite Element spaces with vertex unknowns and flux balances on dual meshes around vertices,
- studies of relationships between FV and Finite Element methods, or mixing of ideas between different families of methods[129, 130, 132, 133],
- Gradient Schemes[55, 69, 76, 77, 79], a generic framework (including HMM methods and some MPFA and DDFV schemes, as well as non-FV methods) for the convergence analysis of numerical methods on numerous models,
- the recent review of Ref. 45 on numerical methods in geosciences.

The overall conclusion of this review is that currently there is no miraculous method which provides an excellent solution in all circumstances. The various numerical methods available for (1.1) should be considered as a kit of clever techniques which can be adapted and re-used in particular situations. The ideas behind the methods are as important as the methods themselves.

Let us close this study with an open question. For the TPFA scheme, the flux balance (1.9) can be written

$$\sum_{L\in\mathcal{M}} \tau_{K,L}(u_K - u_L) = \int_K f(x)\mathrm{d}x, \tag{7.1}$$

with $\tau_{K,L} = \tau_{L,K}$ non-negative and such that the method is coercive. This structure allows one, by using non-linear functions of the solution as test functions, to prove *a priori* estimates and analyse the convergence of the TPFA scheme for non-coercive convection-diffusion equations[35, 49, 56], hyperbolic-parabolic equations[15, 75], equations with Radon measures[57, 84] (used to model wells in reservoirs), or chemotaxis problems[81]. To date, it is not known how to design a method that can be written (7.1) for any mesh and tensor (as separately noticed in Ref. 70), or how to adapt the afore mentioned *a priori* estimate techniques to schemes not having this structure...

**Acknowledgment**

The author would like to thank the following colleagues, whose comments helped improve this paper: D. Di Pietro, M.G. Edwards, R. Eymard, T. Gallouët, F. Hermeline, K. Lipnikov, M. Shashkov, D. Svyatskiy and Yu. Vassilevski. Special thanks to B. Andreianov, R. Herbin, C. Le Potier and G. Manzini for their thorough reading and feedback.

**References**

1. I. Aavatsmark. An introduction to multipoint flux approximations for quadrilateral grids. *Comput. Geosci.*, 6(3-4):405–432, 2002. Locally conservative numerical methods for flow in porous media.
2. I. Aavatsmark, T. Barkve, O. Bøe, and T. Mannseth. Discretization on non-orthogonal, quadrilateral grids for inhomogeneous, anisotropic media. *J. Comput. Phys.*, 127:2–14, 1996.
3. I. Aavatsmark, T. Barkve, O. Bøe, and T. Mannseth. Discretization on unstructured grids for inhomogeneous, anisotropic media. I. Derivation of the methods. *SIAM J. Sci. Comput.*, 19(5):1700–1716 (electronic), 1998.
4. I. Aavatsmark, T. Barkve, O. Bøe, and T. Mannseth. Discretization on unstructured grids for inhomogeneous, anisotropic media. II. Discussion and numerical results. *SIAM J. Sci. Comput.*, 19(5):1717–1736 (electronic), 1998.
5. I. Aavatsmark, G. T. Eigestad, and R. A. Klausen. Numerical convergence of the MPFA O-method for general quadrilateral grids in two and three dimensions. In *Compatible spatial discretizations*, volume 142 of *IMA Vol. Math. Appl.*, pages 1–21. Springer, New York, 2006.
6. I. Aavatsmark, G. T. Eigestad, R. A. Klausen, M. F. Wheeler, and I. Yotov. Convergence of a symmetric MPFA method on quadrilateral grids. *Comput. Geosci.*, 11(4):333–345, 2007.
7. I. Aavatsmark, G. T. Eigestad, B. T. Mallison, and J. M. Nordbotten. A compact multipoint flux approximation method with improved robustness. *Numer. Methods Partial Differential Equations*, 24(5):1329–1360, 2008.
8. I. Aavatsmark, E. Reiso, and R. Teigland. Control-volume discretization method for quadrilateral grids with faults and local refinements. *Comput. Geosci.*, 5:1–23, 2001.
9. B. Abraham and R. Plemmons. *Nonnegative matrices in the mathematical sciences.* Computer Science and Applied Mathematics. Academic Press (Harcourt Brace Jovanovich Publishers), New York, 1979.
10. L. Agélas, D. A. Di Pietro, and J. Droniou. The G method for heteroge-

neous anisotropic diffusion on general meshes. *M2AN Math. Model. Numer. Anal.*, 44(4):597–625, 2010.

11. L. Agelas, R. Eymard, and R. Herbin. A nine-point finite volume scheme for the simulation of diffusion in heterogeneous media. *C. R. Math. Acad. Sci. Paris*, 347(11-12):673–676, 2009.
12. L. Agelas, C. Guichard, and R. Masson. Convergence of finite volume MPFA O type schemes for heterogeneous anisotropic diffusion problems on general meshes. *Int. J. Finite Vol.*, 7(2):33, 2010.
13. B. Andreianov, M. Bendahmane, and F. Hubert. 3d ddfv discretisation of gradient and divergence operators. ii. discrete functional analysis tools and applications to degenerate parabolic problems. 2013. Submitted. http://hal.archives-ouvertes.fr/hal-00567342.
14. B. Andreianov, M. Bendahmane, F. Hubert, and S. Krell. On 3D DDFV discretization of gradient and divergence operators. I. Meshing, operators and discrete duality. *IMA J. Numer. Anal.*, 32(4):1574–1603, 2012.
15. B. Andreianov, M. Bendahmane, and K. H. Karlsen. Discrete duality finite volume schemes for doubly nonlinear degenerate hyperbolic-parabolic equations. *J. Hyperbolic Differ. Equ.*, 7(1):1–67, 2010.
16. B. Andreianov, M. Bendahmane, K. H. Karlsen, and C. Pierre. Convergence of discrete duality finite volume schemes for the cardiac bidomain model. *Netw. Heterog. Media*, 6(2):195–240, 2011.
17. B. Andreianov, F. Boyer, and F. Hubert. Discrete duality finite volume schemes for Leray-Lions-type elliptic problems on general 2D meshes. *Numer. Methods Partial Differential Equations*, 23(1):145–195, 2007.
18. L. Beirão da Veiga. A residual based error estimator for the mimetic finite difference method. *Numer. Math.*, 108(3):387–406, 2008.
19. L. Beirão da Veiga, J. Droniou, and G. Manzini. A unified approach for handling convection terms in finite volumes and mimetic discretization methods for elliptic problems. *IMA J. Numer. Anal.*, 31(4):1357–1401, 2011.
20. L. Beirão da Veiga, K. Lipnikov, and G. Manzini. Convergence analysis of the high-order mimetic finite difference method. *Numer. Math.*, 113(3):325–356, 2009.
21. L. Beirão da Veiga and G. Manzini. An a posteriori error estimator for the mimetic finite difference approximation of elliptic problems. *Internat. J. Numer. Methods Engrg.*, 76(11):1696–1723, 2008.
22. L. Beirão da Veiga and G. Manzini. A higher-order formulation of the mimetic finite difference method. *SIAM J. Sci. Comput.*, 31(1):732–760, 2008.
23. E. Bertolazzi and G. Manzini. A second-order maximum principle preserving finite volume method for steady convection-diffusion problems. *SIAM J. Numer. Anal.*, 43(5):2172–2199 (electronic), 2005.
24. F. Boyer and F. Hubert. Finite volume method for 2D linear and nonlinear elliptic problems with discontinuities. *SIAM J. Numer. Anal.*, 46(6):3032–3070, 2008.
25. F. Brezzi, K. Lipnikov, and M. Shashkov. Convergence of the mimetic finite difference method for diffusion problems on polyhedral meshes. *SIAM J. Numer. Anal.*, 43(5):1872–1896 (electronic), 2005.
26. F. Brezzi, K. Lipnikov, and M. Shashkov. Convergence of mimetic finite difference method for diffusion problems on polyhedral meshes with curved faces. *Math. Models Methods Appl. Sci.*, 16(2):275–297, 2006.
27. F. Brezzi, K. Lipnikov, M. Shashkov, and V. Simoncini. A new discretization methodology for diffusion problems on generalized polyhedral meshes. *Comput. Methods Appl. Mech. Engrg.*, 196(37-40):3682–3692, 2007.

28. F. Brezzi, K. Lipnikov, and V. Simoncini. A family of mimetic finite difference methods on polygonal and polyhedral meshes. *Math. Models Methods Appl. Sci.*, 15(10):1533–1551, 2005.
29. Z. Cai, J. Mandel, and S. Mc Cormick. The finite volume element method for diffusion equations on general triangulations. *SIAM J. Numer. Anal.*, 28(2):392–402, 1991.
30. Z. Q. Cai. On the finite volume element method. *Numer. Math.*, 58(7):713–735, 1991.
31. C. Cancès, M. Cathala, and C. Le Potier. Montone correction for generic cell-centered finite volume approximations of anisotropic diffusion equations. *Numer. Math.*, 125(3):387–417, 2013.
32. A. Cangiani, G. Manzini, and A. Russo. Convergence analysis of the mimetic finite difference method for elliptic problems. *SIAM J. Numer. Anal.*, 47(4):2612–2637, 2009.
33. C. Chainais-Hillairet. Discrete duality finite volume schemes for two-dimensional drift-diffusion and energy-transport models. *Internat. J. Numer. Methods Fluids*, 59(3):239–257, 2009.
34. C. Chainais-Hillairet and J. Droniou. Convergence analysis of a mixed finite volume scheme for an elliptic-parabolic system modeling miscible fluid flows in porous media. *SIAM J. Numer. Anal.*, 45(5):2228–2258 (electronic), 2007.
35. C. Chainais-Hillairet and J. Droniou. Finite-volume schemes for noncoercive elliptic problems with Neumann boundary conditions. *IMA J. Numer. Anal.*, 31(1):61–85, 2011.
36. C. Chainais-Hillairet, S. Krell, and A. Mouton. Study of discrete duality finite volume schemes for the peaceman model. 2013. Submitted. http://hal.archives-ouvertes.fr/hal-00790449.
37. Q.-Y. Chen, J. Wan, Y. Yang, and R. T. Mifflin. Enriched multi-point flux approximation for general grids. *J. Comput. Phys.*, 227(3):1701–1721, 2008.
38. Y. Coudière and F. Hubert. A 3D discrete duality finite volume method for nonlinear elliptic equations. *SIAM J. Sci. Comput.*, 33(4):1739–1764, 2011.
39. Y. Coudière, F. Hubert, and G. Manzini. A CeVeFE DDFV scheme for discontinuous anisotropic permeability tensors. In *Finite volumes for complex applications VI - Problems & Perspectives*, volume 4 of *Springer Proc. Math.*, pages 283–291. Springer, Heidelberg, 2011.
40. Y. Coudière and G. Manzini. The discrete duality finite volume method for convection-diffusion problems. *SIAM J. Numer. Anal.*, 47(6):4163–4192, 2010.
41. Y. Coudière, C. Pierre, O. Rousseau, and R. Turpault. A 2D/3D discrete duality finite volume scheme. Application to ECG simulation. *Int. J. Finite Vol.*, 6(1):24, 2009.
42. Y. Coudière, J.-P. Vila, and P. Villedieu. Convergence rate of a finite volume scheme for a two-dimensional convection-diffusion problem. *M2AN Math. Model. Numer. Anal.*, 33(3):493–516, 1999.
43. A. A. Danilov and Y. V. Vassilevski. A monotone nonlinear finite volume method for diffusion equations on conformal polyhedral meshes. *Russian J. Numer. Anal. Math. Modelling*, 24(3):207–227, 2009.
44. S. Delcourte, K. Domelevo, and P. Omnes. A discrete duality finite volume approach to Hodge decomposition and div-curl problems on almost arbitrary two-dimensional meshes. *SIAM J. Numer. Anal.*, 45(3):1142–1174, 2007.
45. D. Di Pietro and M. Vohralik. A review of recent advances in discretization methods, a posteriori error analysis, and adaptive algorithms for numerical modeling in geosciences. 2013. To appear in Oil & Gas Science and Technology. DOI: 10.2516/ogst/2013158.

46. D. A. Di Pietro. Cell centered galerkin methods for diffusive problems. *M2AN Math. Model. Numer. Anal.*, 46(1):111–144, 2012.
47. D. A. Di Pietro. On the conservativity of cell centered galerkin methods. *C. R. Math. Acad. Sci. Paris, Ser. I*, 351(3-4):155–159, 2013.
48. K. Domelevo and P. Omnes. A finite volume method for the Laplace equation on almost arbitrary two-dimensional grids. *M2AN Math. Model. Numer. Anal.*, 39(6):1203–1249, 2005.
49. J. Droniou. Error estimates for the convergence of a finite volume discretization of convection-diffusion equations. *J. Numer. Math.*, 11(1):1–32, 2003.
50. J. Droniou. Finite volume schemes for fully non-linear elliptic equations in divergence form. *M2AN Math. Model. Numer. Anal.*, 40(6):1069–1100 (2007), 2006.
51. J. Droniou. Remarks on discretizations of convection terms in hybrid mimetic mixed methods. *Netw. Heterog. Media*, 5(3):545–563, 2010.
52. J. Droniou and R. Eymard. A mixed finite volume scheme for anisotropic diffusion problems on any grid. *Numer. Math.*, 105(1):35–71, 2006.
53. J. Droniou and R. Eymard. Study of the mixed finite volume method for Stokes and Navier-Stokes equations. *Numer. Methods Partial Differential Equations*, 25(1):137–171, 2009.
54. J. Droniou, R. Eymard, T. Gallouët, and R. Herbin. A unified approach to mimetic finite difference, hybrid finite volume and mixed finite volume methods. *Math. Models Methods Appl. Sci.*, 20(2):265–295, 2010.
55. J. Droniou, R. Eymard, T. Gallouët, and R. Herbin. Gradient schemes: a generic framework for the discretisation of linear, nonlinear and nonlocal elliptic and parabolic equations. *Math. Models Methods Appl. Sci. (M3AS)*, 23(13):2395–2432, 2012. DOI: 10.1142/S0218202513500358.
56. J. Droniou and T. Gallouët. Finite volume methods for convection-diffusion equations with right-hand side in $H^{-1}$. *M2AN Math. Model. Numer. Anal.*, 36(4):705–724, 2002.
57. J. Droniou, T. Gallouët, and R. Herbin. A finite volume scheme for a noncoercive elliptic equation with measure data. *SIAM J. Numer. Anal.*, 41(6):1997–2031 (electronic), 2003.
58. J. Droniou and C. Le Potier. Construction and convergence study of schemes preserving the elliptic local maximum principle. *SIAM J. Numer. Anal.*, 49(2):459–490, 2011.
59. M. Edwards and C. Rogers. A flux continuous scheme for the full tensor pressure equation. In *Proc. of the 4th European Conf. on the Mathematics of Oil Recovery*, volume D, Røros, Norway, 1994.
60. M. Edwards and H. Zheng. A quasi-positive family of continuous darcy-flux finite-volume schemes with full pressure support. *J. Comput. Phys.*, 227:9333–9364, 2008.
61. M. G. Edwards. Unstructured, control-volume distributed, full-tensor finite-volume schemes with flow based grids. *Comput. Geosci.*, 6(3-4):433–452, 2002. Locally conservative numerical methods for flow in porous media.
62. M. G. Edwards and M. Pal. Positive-definite $q$-families of continuous subcell Darcy-flux CVD(MPFA) finite-volume schemes and the mixed finite element method. *Internat. J. Numer. Methods Fluids*, 57(4):355–387, 2008.
63. M. G. Edwards and C. F. Rogers. Finite volume discretization with imposed flux continuity for the general tensor pressure equation. *Comput. Geosci.*, 2(4):259–290, 1998.
64. M. G. Edwards and H. Zheng. Double-families of quasi-positive Darcy-flux approximations with highly anisotropic tensors on structured and unstructured grids. *J.*

*Comput. Phys.*, 229(3):594–625, 2010.

65. M. G. Edwards and H. Zheng. Quasi $M$-matrix multifamily continuous Darcy-flux approximations with full pressure support on structured and unstructured grids in three dimensions. *SIAM J. Sci. Comput.*, 33(2):455–487, 2011.
66. G. T. Eigestad, I. Aavatsmark, and M. Espedal. Symmetry and $M$-matrix issues for the $O$-method on an unstructured grid. *Comput. Geosci.*, 6(3-4):381–404, 2002. Locally conservative numerical methods for flow in porous media.
67. G. T. Eigestad and R. A. Klausen. On the convergence of the multi-point flux approximation O-method: numerical experiments for discontinuous permeability. *Numer. Methods Partial Differential Equations*, 21(6):1079–1098, 2005.
68. R. E. Ewing, T. Lin, and Y. Lin. On the accuracy of the finite volume element method based on piecewise linear polynomials. *SIAM J. Numer. Anal.*, 39(6):1865–1888, 2002.
69. R. Eymard, P. Féron, T. Gallouët, R. Herbin, and C. Guichard. Gradient schemes for the stefan problem. *IJFV International Journal On Finite Volumes*, 10, 2013.
70. R. Eymard, T. Gallouët, D. Guichard, R. Herbin, and R. Masson. TP or not TP, that is the question. *Computational Geosciences*, pages 1–12, 2014.
71. R. Eymard, T. Gallouët, and R. Herbin. Finite volume methods. In P. G. Ciarlet and J.-L. Lions, editors, *Techniques of Scientific Computing, Part III*, Handbook of Numerical Analysis, VII, pages 713–1020. North-Holland, Amsterdam, 2000.
72. R. Eymard, T. Gallouët, and R. Herbin. Benchmark on anisotropic problems, sushi: a scheme using stabilization and hybrid interfaces for anisotropic heterogeneous diffusion problems. In *Finite volumes for complex applications V*, pages 801–814. ISTE, London, 2008.
73. R. Eymard, T. Gallouët, and R. Herbin. Cell centred discretisation of non linear elliptic problems on general multidimensional polyhedral grids. *J. Numer. Math.*, 17(3):173–193, 2009.
74. R. Eymard, T. Gallouët, and R. Herbin. Discretization of heterogeneous and anisotropic diffusion problems on general nonconforming meshes SUSHI: a scheme using stabilization and hybrid interfaces. *IMA J. Numer. Anal.*, 30(4):1009–1043, 2010.
75. R. Eymard, T. Gallouët, R. Herbin, and A. Michel. Convergence of a finite volume scheme for nonlinear degenerate parabolic equations. *Numer. Math.*, 92(1):41–82, 2002.
76. R. Eymard, C. Guichard, and R. Herbin. Small-stencil 3D schemes for diffusive flows in porous media. *ESAIM Math. Model. Numer. Anal.*, 46(2):265–290, 2012.
77. R. Eymard, A. Handlovičová, R. Herbin, K. Mikula, and O. Stašová. Gradient schemes for image processing. In *Finite volumes for complex applications VI - Problems & Perspectives*, volume 4 of *Springer Proc. Math.*, pages 429–437. Springer, Heidelberg, 2011.
78. R. Eymard, G. Henry, R. Herbin, F. Hubert, R. Klöfkorn, and G. Manzini. 3d benchmark on discretization schemes for anisotropic diffusion problems on general grids. In *Finite volumes for complex applications VI - Problems & Perspectives*, volume 4 of *Springer Proceedings in Mathematics*, pages 895–930. Springer, Heidelberg, 2011.
79. R. Eymard and R. Herbin. Gradient scheme approximations for diffusion problems. In *Finite volumes for complex applications VI - Problems & Perspectives*, volume 4 of *Springer Proc. Math.*, pages 439–447. Springer, Heidelberg, 2011.
80. I. Faille. A control volume method to solve an elliptic equation on a two-dimensional irregular mesh. *Computer methods in applied mechanics and engineering*, 100(2):275–290, 1992.

81. F. Filbet. A finite volume scheme for the patlak-keller-segel chemotaxis model. *Numer. Math.*, 104:457–488, 2006.
82. H. A. Friis and M. G. Edwards. A family of MPFA finite-volume schemes with full pressure support for the general tensor pressure equation on cell-centered triangular grids. *J. Comput. Phys.*, 230(1):205–231, 2011.
83. H. A. Friis, M. G. Edwards, and J. Mykkeltveit. Symmetric positive definite flux-continuous full-tensor finite-volume schemes on unstructured cell-centered triangular grids. *SIAM J. Sci. Comput.*, 31(2):1192–1220, 2008/09.
84. T. Gallouët and R. Herbin. Finite volume approximation of elliptic problems with irregular data. In *Finite volumes for complex applications II*, pages 155–162. Hermes Sci. Publ., Paris, 1999.
85. V. Gyrya and K. Lipnikov. High-order mimetic finite difference method for diffusion problems on polygonal meshes. *J. Comput. Phys.*, 227(20):8841–8854, 2008.
86. R. Herbin. An error estimate for a finite volume scheme for a diffusion–convection problem on a triangular mesh. *Numerical Methods for Partial Differential Equations*, 11(2):165–173, 1995.
87. R. Herbin and F. Hubert. Benchmark on discretization schemes for anisotropic diffusion problems on general grids. In *Finite volumes for complex applications V*, pages 659–692. ISTE, London, 2008.
88. F. Hermeline. Une méthode de volumes finis pour les équations elliptiques du second ordre. *C. R. Acad. Sci. Paris Sér. I Math.*, 326(12):1433–1436, 1998.
89. F. Hermeline. A finite volume method for the approximation of diffusion operators on distorted meshes. *J. Comput. Phys.*, 160(2):481–499, 2000.
90. F. Hermeline. Approximation of diffusion operators with discontinuous tensor coefficients on distorted meshes. *Comput. Methods Appl. Mech. Engrg.*, 192(16-18):1939–1959, 2003.
91. F. Hermeline. Approximating second-order vector differential operators on distorted meshes in two space dimensions. *Internat. J. Numer. Methods Engrg.*, 76(7):1065–1089, 2008.
92. F. Hermeline. A finite volume method for approximating 3D diffusion operators on general meshes. *J. Comput. Phys.*, 228(16):5763–5786, 2009.
93. F. Hermeline. A finite volume method for the approximation of convection-diffusion equations on general meshes. *Internat. J. Numer. Methods Engrg.*, 91(12):1331–1357, 2012.
94. E. Hopf. Elementare bemerkungen ber die lsungen partieller differentialgleichungen zweiter ordnung vom elliptischen typus. *Sitzungsberichte der Berliner Akademie der Wissenschaften*, 19:147–152, 1927.
95. I. V. Kapyrin. A family of monotone methods for the numerical solution of three-dimensional diffusion problems on unstructured tetrahedral meshes. *Dokl. Akad. Nauk*, 416(5):588–593, 2007.
96. E. Keilegavlen, J. M. Nordbotten, and I. Aavatsmark. Sufficient criteria are necessary for monotone control volume methods. *Appl. Math. Lett.*, 22(8):1178–1180, 2009.
97. D. S. Kershaw. Differencing of the diffusion equation in Lagrangian hydrodynamic codes. *J. Comput. Phys.*, 39(2):375–395, 1981.
98. R. A. Klausen and A. F. Stephansen. Convergence of multi-point flux approximations on general grids and media. *Int. J. Numer. Anal. Model.*, 9(3):584–606, 2012.
99. R. A. Klausen and R. Winther. Convergence of multipoint flux approximations on quadrilateral grids. *Numer. Methods Partial Differential Equations*, 22(6):1438–1454, 2006.
100. S. Krell. Stabilized DDFV schemes for Stokes problem with variable viscosity on

general 2D meshes. *Numer. Methods Partial Differential Equations*, 27(6):1666–1706, 2011.

101. S. Krell and G. Manzini. The discrete duality finite volume method for Stokes equations on three-dimensional polyhedral meshes. *SIAM J. Numer. Anal.*, 50(2):808–837, 2012.
102. C. Le Potier. A finite volume method for the approximation of highly anisotropic diffusion operators on unstructured meshes. In *Finite volumes for complex applications IV*, pages 401–412. ISTE, London, 2005.
103. C. Le Potier. Schéma volumes finis monotone pour des opérateurs de diffusion fortement anisotropes sur des maillages de triangles non structurés. *C. R. Math. Acad. Sci. Paris*, 341(12):787–792, 2005.
104. C. Le Potier. Finite volume scheme satisfying maximum and minimum principles for anisotropic diffusion operators. In *Finite volumes for complex applications V*, pages 103–118. ISTE, London, 2008.
105. C. Le Potier. A nonlinear finite volume scheme satisfying maximum and minimum principles for diffusion operators. *Int. J. Finite Vol.*, 6(2):20, 2009.
106. C. Le Potier. Un schéma linéaire vérifiant le principe du maximum pour des opérateurs de diffusion très anisotropes sur des maillages déformés. *C. R. Math. Acad. Sci. Paris*, 347(1-2):105–110, 2009.
107. C. Le Potier. Correction non linéaire et principe du maximum pour la discrétisation d'opérateurs de diffusion avec des schémas volumes finis centrés sur les mailles. *C. R. Math. Acad. Sci. Paris*, 348(11-12):691–695, 2010.
108. C. Le Potier. private communication, 2013.
109. C. Le Potier and A. Mahamane. Correction non linéaire et principe du maximum avec des schémas hybrides pour la discrétisation d'opérateurs de diffusion. *C. R. Math. Acad. Sci. Paris*, 350(1-2):101–106, 2012.
110. K. Lipnikov. private communication, 2013.
111. K. Lipnikov, G. Manzini, and M. Shashkov. Mimetic finite difference method. Technical Report LAUR-12-24245, Los Alamos National Laboratory, 2012.
112. K. Lipnikov, G. Manzini, and D. Svyatskiy. Analysis of the monotonicity conditions in the mimetic finite difference method for elliptic problems. *J. Comput. Phys.*, 230(7):2620–2642, 2011.
113. K. Lipnikov, G. Manzini, and D. Svyatskiy. Monotonicity conditions in the mimetic finite difference method. In *Finite volumes for complex applications VI - Problems & Perspectives*, volume 4 of *Springer Proc. Math.*, pages 653–661. Springer, Heidelberg, 2011.
114. K. Lipnikov, M. Shashkov, and D. Svyatskiy. The mimetic finite difference discretization of diffusion problem on unstructured polyhedral meshes. *J. Comput. Phys.*, 211(2):473–491, 2006.
115. K. Lipnikov, M. Shashkov, D. Svyatskiy, and Y. Vassilevski. Monotone finite volume schemes for diffusion equations on unstructured triangular and shape-regular polygonal meshes. *J. Comput. Phys.*, 227(1):492–512, 2007.
116. K. Lipnikov, M. Shashkov, and I. Yotov. Local flux mimetic finite difference methods. *Numer. Math.*, 112(1):115–152, 2009.
117. K. Lipnikov, D. Svyatskiy, and Y. Vassilevski. Interpolation-free monotone finite volume method for diffusion equations on polygonal meshes. *J. Comput. Phys.*, 228(3):703–716, 2009.
118. K. Lipnikov, D. Svyatskiy, and Y. Vassilevski. A monotone finite volume method for advection-diffusion equations on unstructured polygon meshes. *J. Comput. Phys.*, 229(11):4017–4032, 2010.

119. K. Lipnikov, D. Svyatskiy, and Y. Vassilevski. Minimal stencil finite volume scheme with the discrete maximum principle. *Russian J. Numer. Anal. Math. Modelling*, 27(4):369–385, 2012.
120. C. Miranda. *Partial differential equations of elliptic type.* Ergebnisse der Mathematik und ihrer Grenzgebiete, Band 2. Springer-Verlag, New York, 1970. Second revised edition. Translated from the Italian by Zane C. Motteler.
121. K. Nikitin and Y. Vassilevski. A monotone nonlinear finite volume method for advection-diffusion equations on unstructured polyhedral meshes in 3D. *Russian J. Numer. Anal. Math. Modelling*, 25(4):335–358, 2010.
122. J. M. Nordbotten and I. Aavatsmark. Monotonicity conditions for control volume methods on uniform parallelogram grids in homogeneous media. *Comput. Geosci.*, 9(1):61–72, 2005.
123. J. M. Nordbotten, I. Aavatsmark, and G. T. Eigestad. Monotonicity of control volume methods. *Numer. Math.*, 106(2):255–288, 2007.
124. M. Pal and M. G. Edwards. A family of multi-point flux approximation schemes for general element types in two and three dimensions with convergence performance. *Internat. J. Numer. Methods Fluids*, 69(11):1797–1817, 2012.
125. M. Pal, M. G. Edwards, and A. R. Lamb. Convergence study of a family of flux-continuous, finite-volume schemes for the general tensor pressure equation. *Internat. J. Numer. Methods Fluids*, 51(9-10):1177–1203, 2006.
126. Z. Sheng and G. Yuan. The finite volume scheme preserving extremum principle for diffusion equations on polygonal meshes. *J. Comput. Phys.*, 230(7):2588–2604, 2011.
127. Z. Sheng and G. Yuan. An improved monotone finite volume scheme for diffusion equation on polygonal meshes. *J. Comput. Phys.*, 231(9):3739–3754, 2012.
128. N. Tan Trung. A study of finite volume scheme for diffusion operators. Master thesis, CEA, France, 2009.
129. M. Vohralík. Equivalence between lowest-order mixed finite element and multi-point finite volume methods on simplicial meshes. *M2AN Math. Model. Numer. Anal.*, 40(2):367–391, 2006.
130. M. Vohralk and B. Wohlmuth. Mixed finite element methods: implementation with one unknown per element, local flux ex- pressions, positivity, polygonal meshes, and relations to other methods. *Math. Models Methods Appl. Sci.*, 23(5):803–838, 2013. DOI: 10.1142/S021820251230061.
131. S. Wang, G. Yuan, Y. Li, and Z. Sheng. A monotone finite volume scheme for advection-diffusion equations on distorted meshes. *Internat. J. Numer. Methods Fluids*, 69(7):1283–1298, 2012.
132. M. F. Wheeler and I. Yotov. A multipoint flux mixed finite element method. *SIAM J. Numer. Anal.*, 44(5):2082–2106 (electronic), 2006.
133. A. Younès, P. Ackerer, and G. Chavent. From mixed finite elements to finite volumes for elliptic PDEs in two and three dimensions. *Internat. J. Numer. Methods Engrg.*, 59(3):365–388, 2004.
134. G. Yuan and Z. Sheng. Monotone finite volume schemes for diffusion equations on polygonal meshes. *J. Comput. Phys.*, 227(12):6288–6312, 2008.